Cell Reports, Volume *42*

Supplemental information

Tcf21 marks visceral adipose mesenchymal progenitors and functions as a rate-limiting factor during visceral adipose tissue development

Qianglin Liu, Chaoyang Li, Buhao Deng, Peidong Gao, Leshan Wang, Yuxia Li, Mohammad Shiri, Fozi Alkaifi, Junxing Zhao, Jacqueline M. Stephens, Constantine A. Simintiras, Joseph Francis, Jiangwen Sun, and Xing Fu

Cell Reports, Volume ■ ■

Supplemental information

Tcf21 marks visceral adipose mesenchymal progenitors and functions as a rate-limiting factor during visceral adipose tissue development

Qianglin Liu, Chaoyang Li, Buhao Deng, Peidong Gao, Leshan Wang, Yuxia Li, Mohammad Shiri, Fozi Alkaifi, Junxing Zhao, Jacqueline M. Stephens, Constantine A. Simintiras, Joseph Francis, Jiangwen Sun, and Xing Fu

SUPPLEMENTAL FIGURES

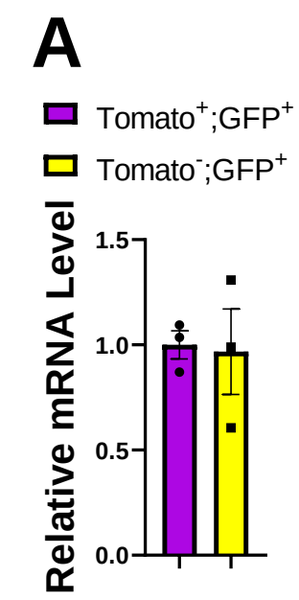

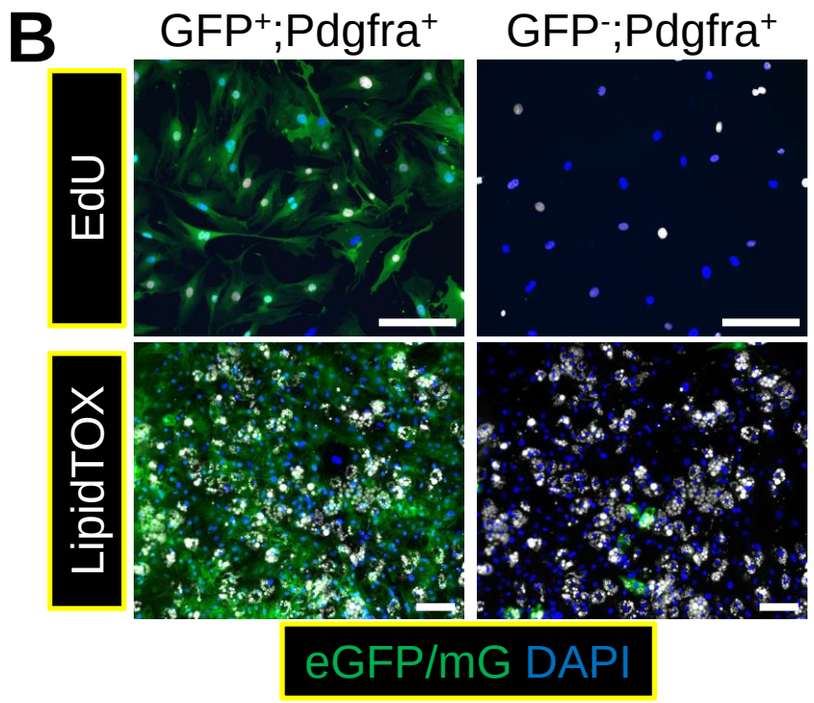

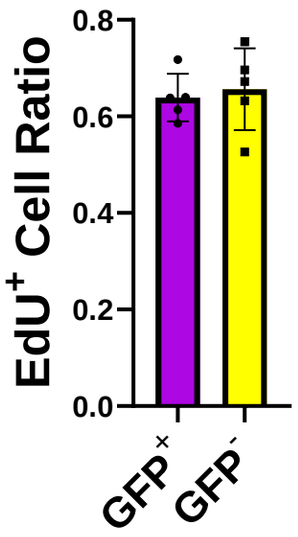

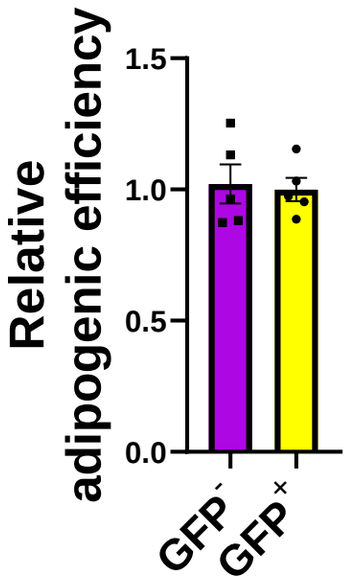

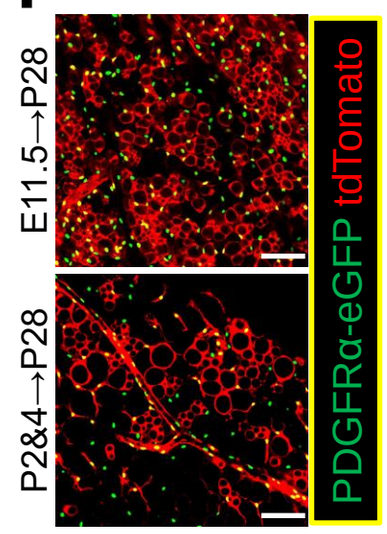

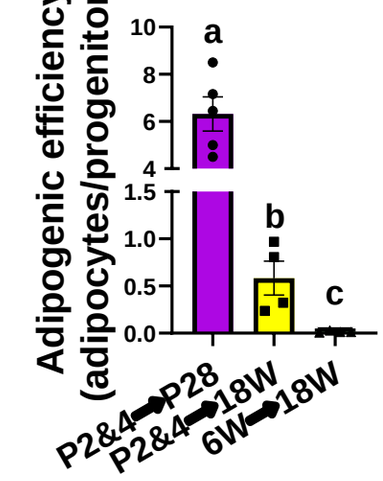

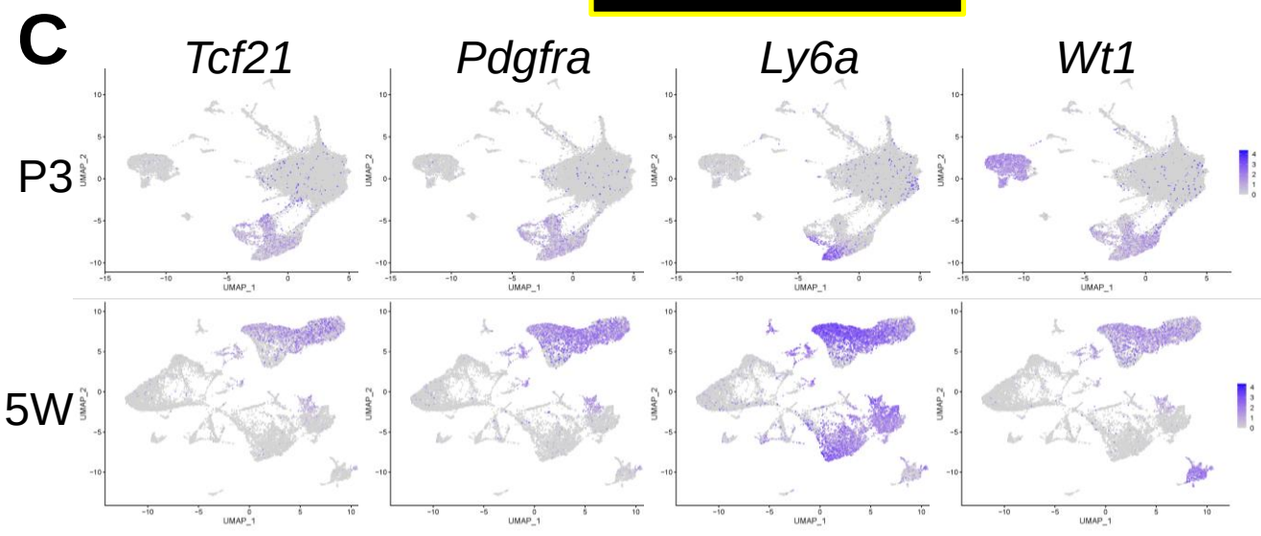

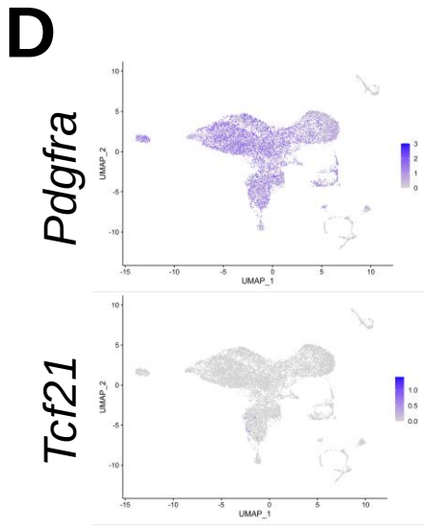

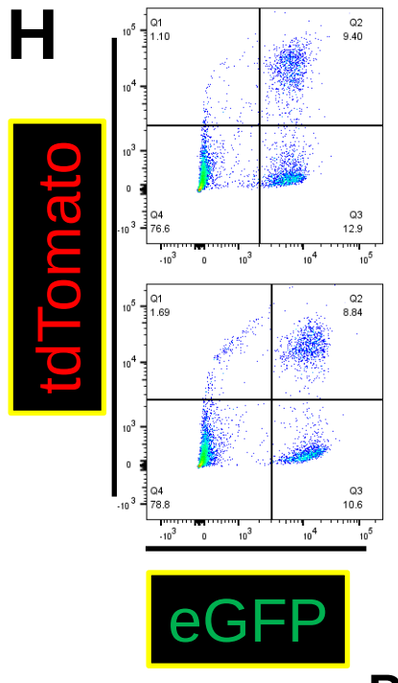

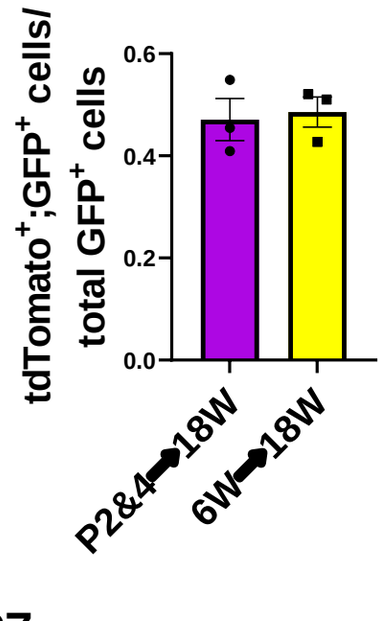

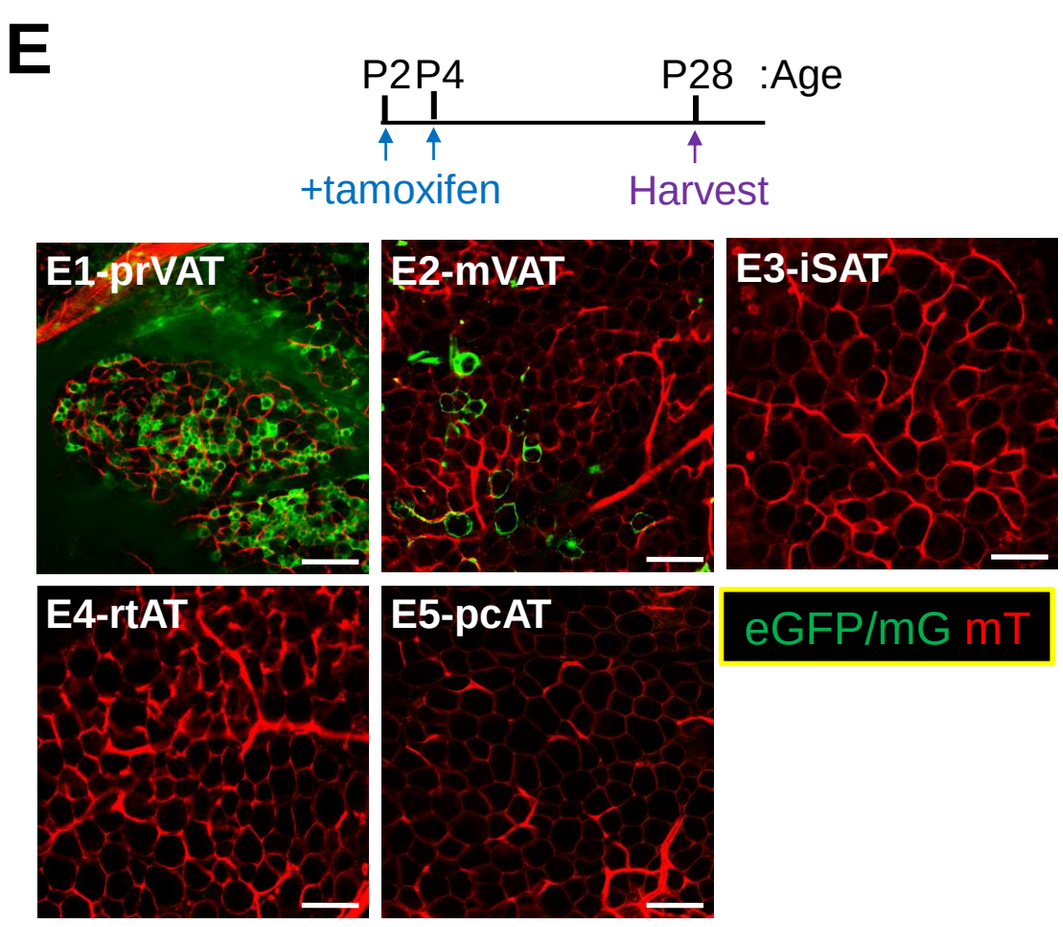

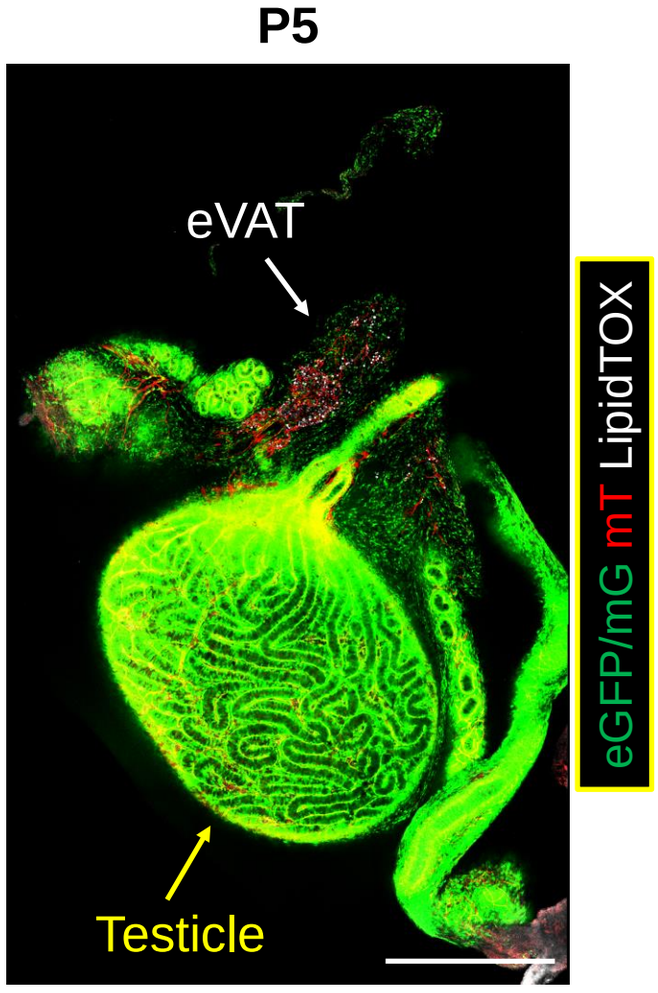

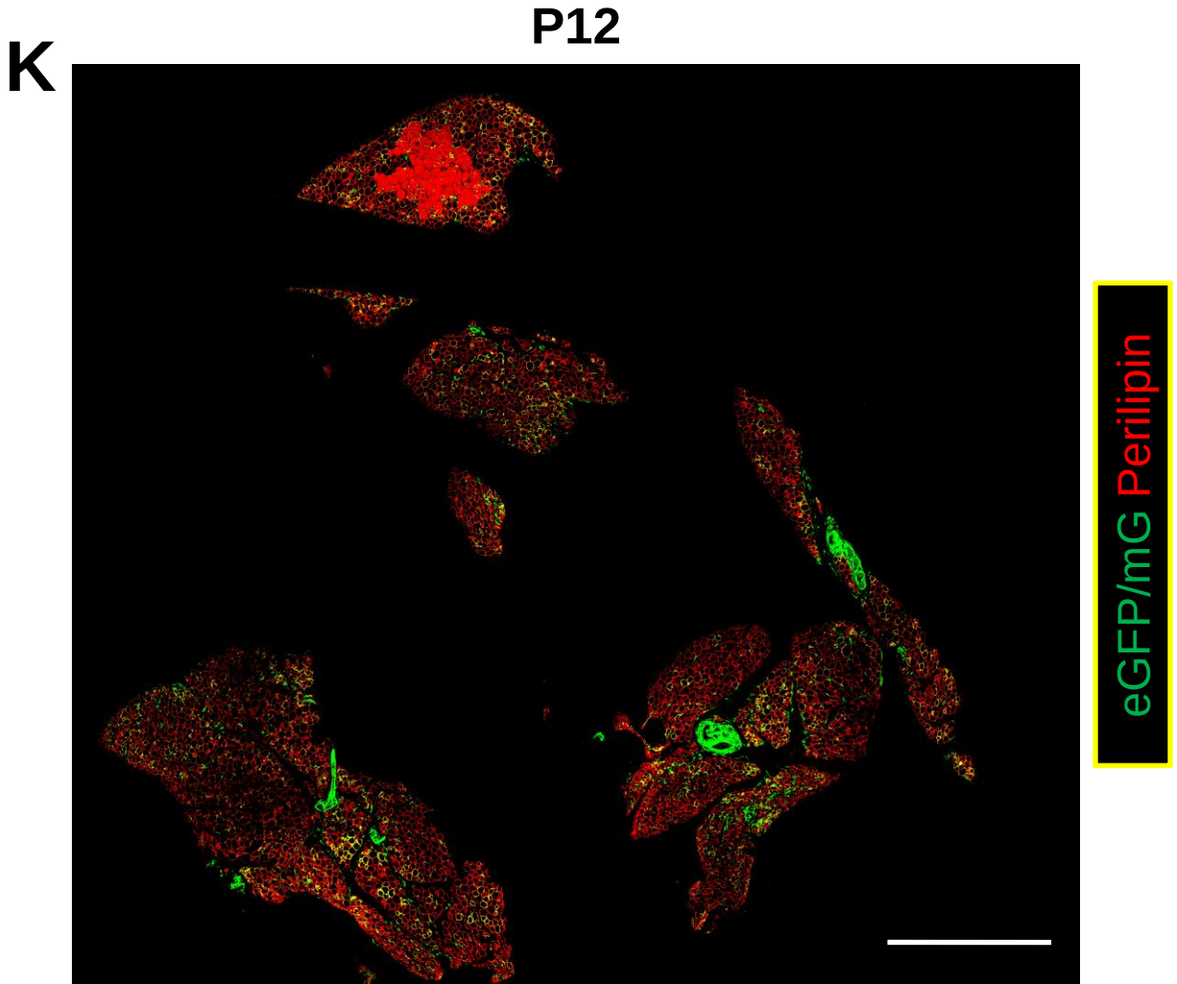

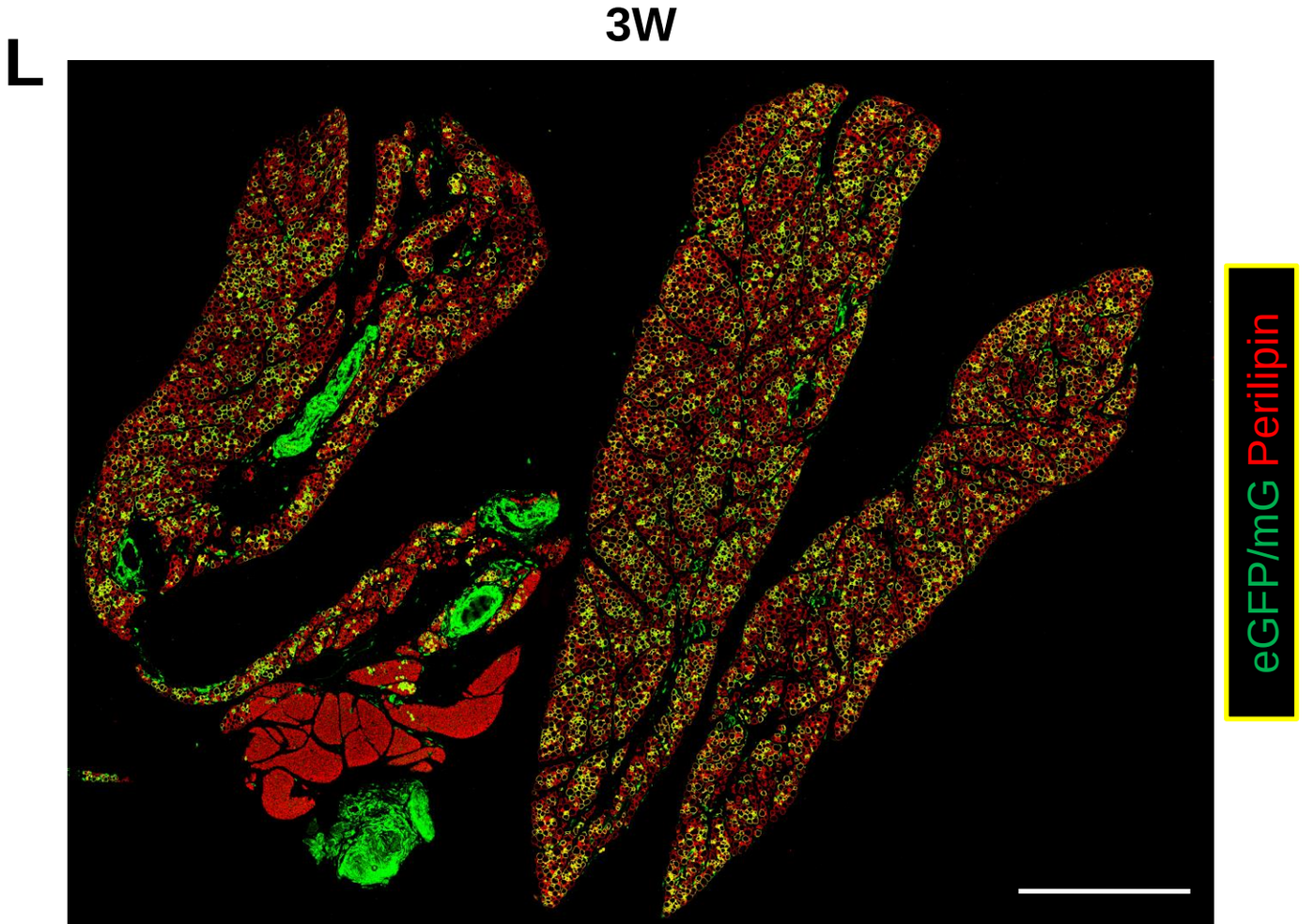

Figure S1 (Related Figure 1). ***Tcf21* lineage cells give rise to visceral adipocytes.** (**A**) The expression of *Tcf21* in tdTomato^{+};GFP^{+} and tdTomato^{-};GFP^{+} cells isolated from 3W *Tcf21*$^{MCM/+}$;*R26*^{tdTomato};*Pdgfra*^{eGFP} mice that were treated with TM at P2 and 4 was measured by realtime PCR. n=3; unpaired *t*-test. (**B**) GFP^{+};Pdgfra^{+} and GFP^{-};Pdgfra^{+} isolated from 3W *Tcf21*$^{MCM/+}$;*R26*$^{eGFP/mTmG}$ treated with TM on P2 and 4 were subjected to an EdU-based proliferation assay or adipogenic induction. The proliferation rates and adipogenic efficiencies were measured. Scale bar=50μm. n=5; unpaired *t*-test. (**C**) UMAP graphs show the expression of select genes in cells isolated from eVAT of WT C57BL/6 mice at P3 or 5W of age. (**D**) UMAP graphs show the expression of select genes in cells isolated from iSAT of WT C57BL/6 mice at P12 of age. (**E**)*Tcf21* LT mice were treated with TM on P2 and P4, followed by sample collection at P28. Representative whole-mount confocal microscopic images show the presence of *Tcf21* lineage ACs in prVAT (**E1**), and mVAT (**E2**), but not in iSAT (**E3**), rtAT (**E4**), or pcAT (**E5**). (**F**) Whole-mount images of eVAT from P28 *Tcf21*$^{MCM/+}$;*R26*^{tdTomato};*Pdgfra*^{eGFP} mice treated TM at E11.5 or P2 and 4. Scale bar=100μm. (**G**) The relative adipogenic efficiencies of *Tcf21* LCs (the ratio between *Tcf21* lineage-traced adipocytes and progenitor cells) in Figures 1H-J were measured. n=4 or 5; one-way ANOVA. Different letters indicate significant differences (p<0.05). (**H**) The fractions of tdTomato^{+} cells in total Pdgfra-eGFP^{+} cells of *Tcf21*$^{MCM/+}$;*R26*^{tdTomato};*Pdgfra*^{eGFP} mice that were treated with TM at P2 and 4 or 6W and fed with HFD for 12W starting at 6W were measured by FC. n=3; unpaired *t*-test. (**I**-**L**) *Tcf21* LT mice treated with TM at P2 and P4 were euthanized at P5 (**I**), P7 (**J**), P12 (**K**), or 3W (**L**). eVAT samples were either stained with LipidTOX and analyzed by whole-mount confocal microscopic imaging (**I**-**J**) or sectioned and analyzed by IHC using antibodies against GFP and Perilipin (**K**-**L**). Scale bar=1 mm. Data are represented as mean ± SEM.

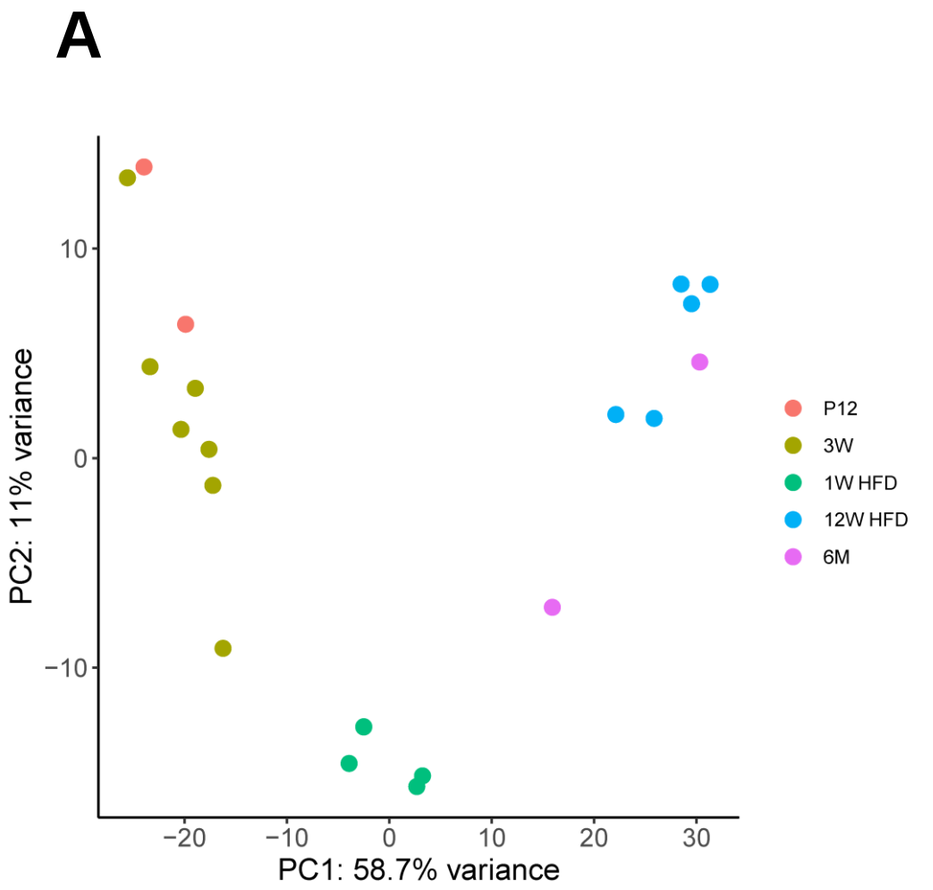
A
PC2: 11% variance
PC1: 58.7% variance
P12
3W
1W HFD
12W HFD
6M

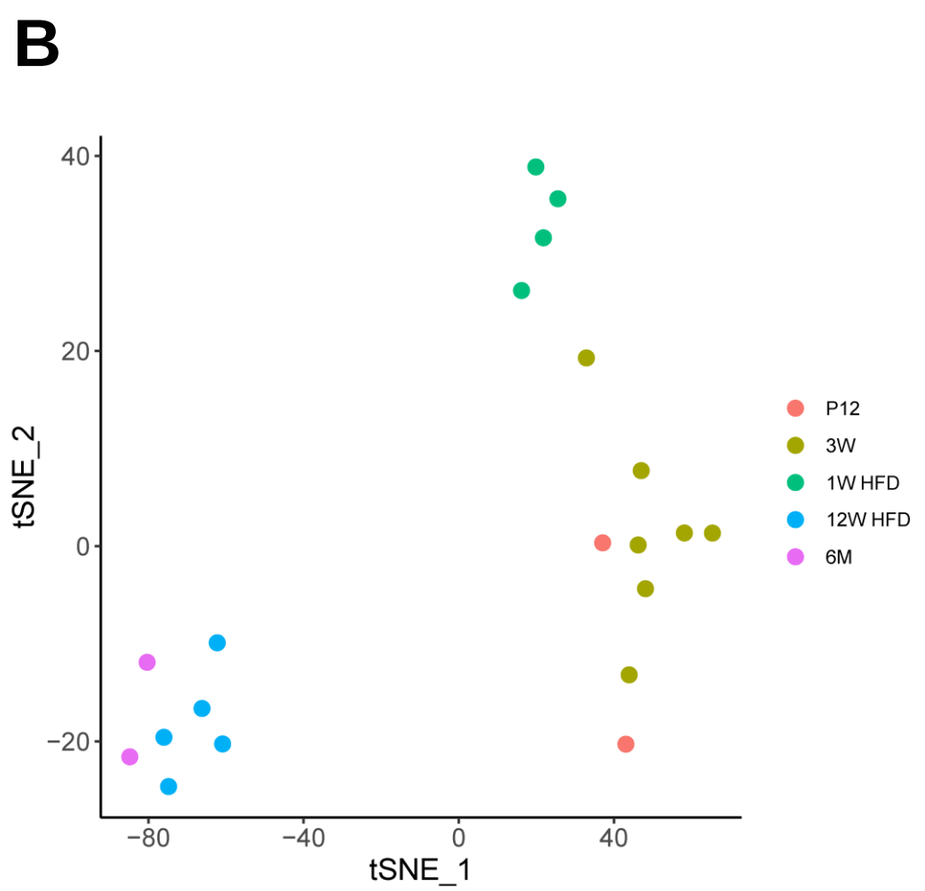
B
tSNE_2
tSNE_1
P12
3W
1W HFD
12W HFD
6M

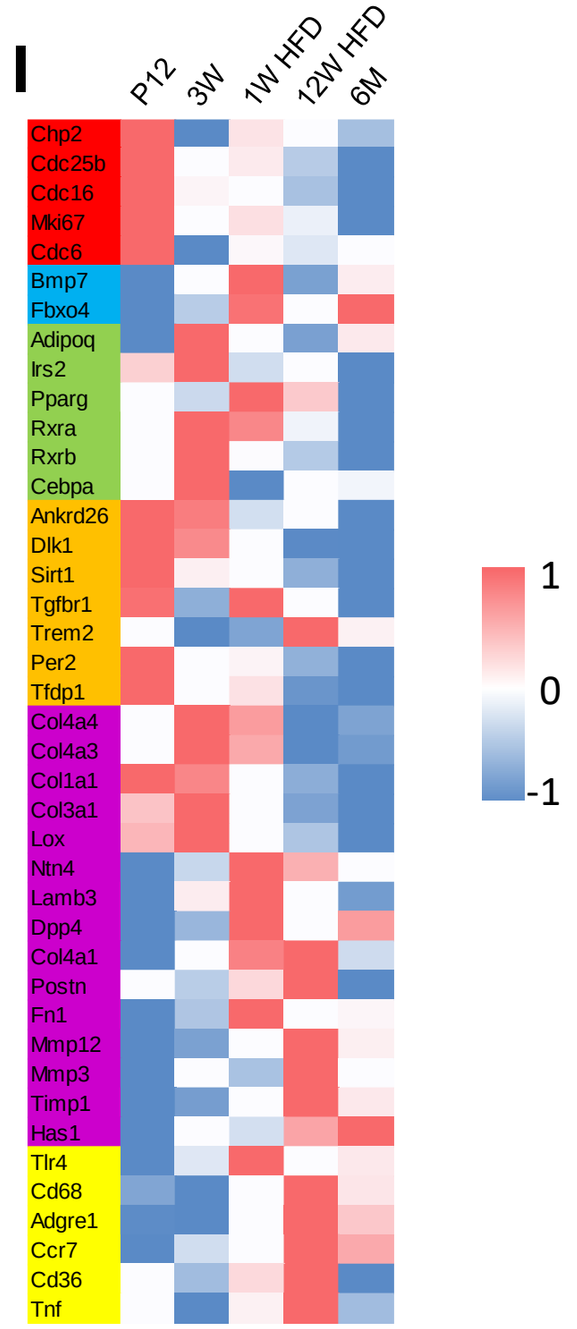
I
P12
3W
1W HFD
12W HFD
6M
Chp2
Cdc25b
Cdc16
Mki67
Cdc6
Bmp7
Fbxo4
Adipoq
Irs2
Pparg
Rxra
Rxrb
Cebpa
Ankrd26
Dlk1
Sirt1
Tgfbr1
Trem2
Per2
Tfdp1
Col4a4
Col4a3
Col1a1
Col3a1
Lox
Ntn4
Lamb3
Dpp4
Col4a1
Postn
Fn1
Mmp12
Mmp3
Timp1
Has1
Tlr4
Cd68
Adgre1
Ccr7
Cd36
Tnf
1
0
-1

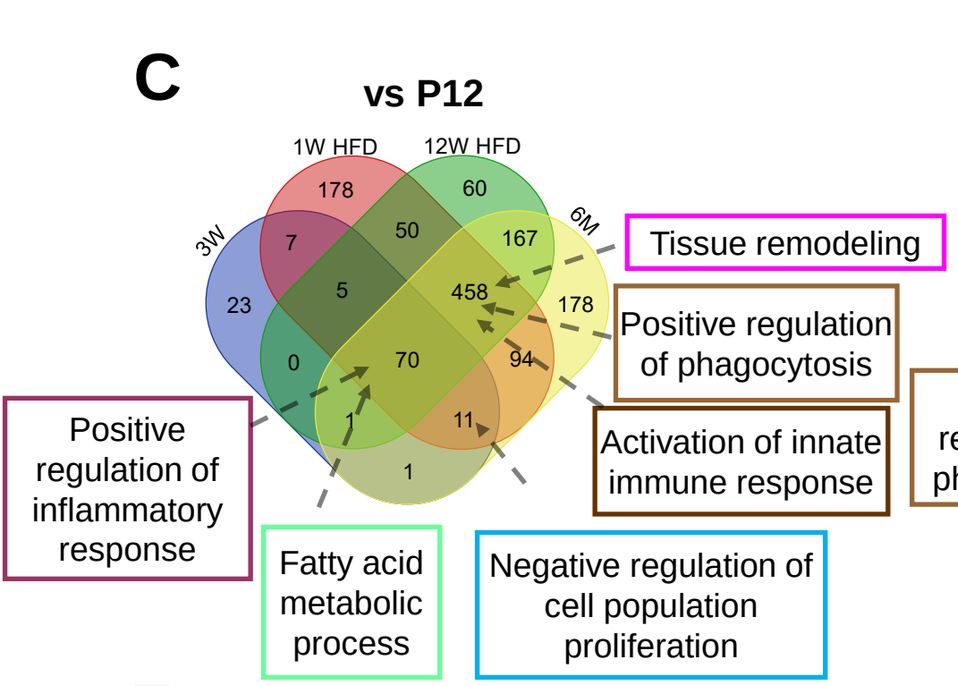
C
vs P12
1W HFD
12W HFD
3W
6M
178
60
7
50
167
23
5
458
178
0
70
94
1
11
1
Tissue remodeling
Positive regulation of phagocytosis
Activation of innate immune response
Positive regulation of inflammatory response
Fatty acid metabolic process
Negative regulation of cell population proliferation

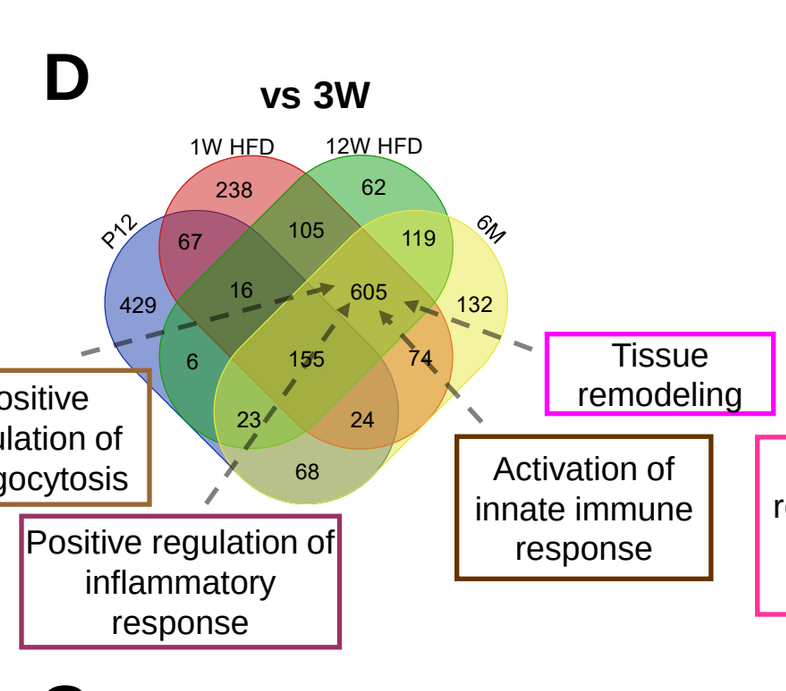
D
vs 3W
1W HFD
12W HFD
P12
6M
238
62
67
105
119
429
16
605
132
6
155
74
23
24
68
Positive regulation of phagocytosis
Tissue remodeling
Activation of innate immune response
Positive regulation of inflammatory response

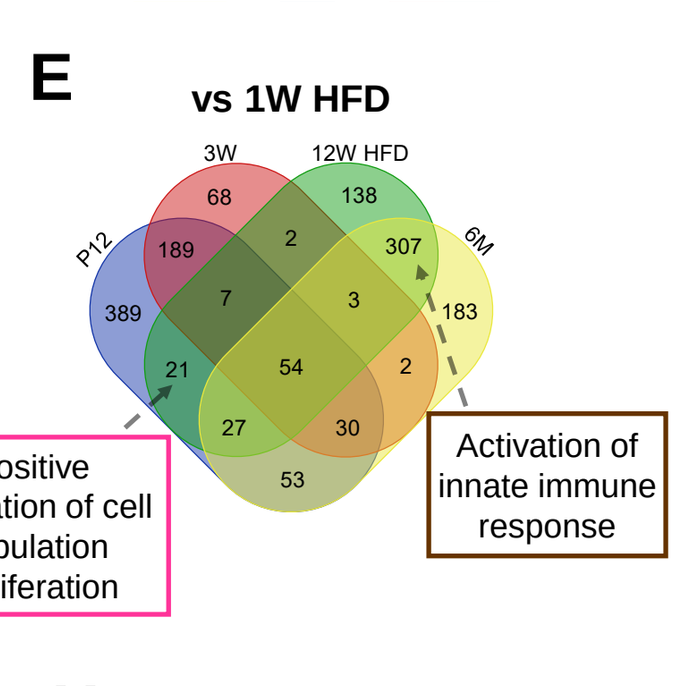
E
vs 1W HFD
3W
12W HFD
P12
6M
68
138
189
2
307
389
7
3
183
21
54
2
27
30
53
Positive regulation of cell population proliferation
Activation of innate immune response

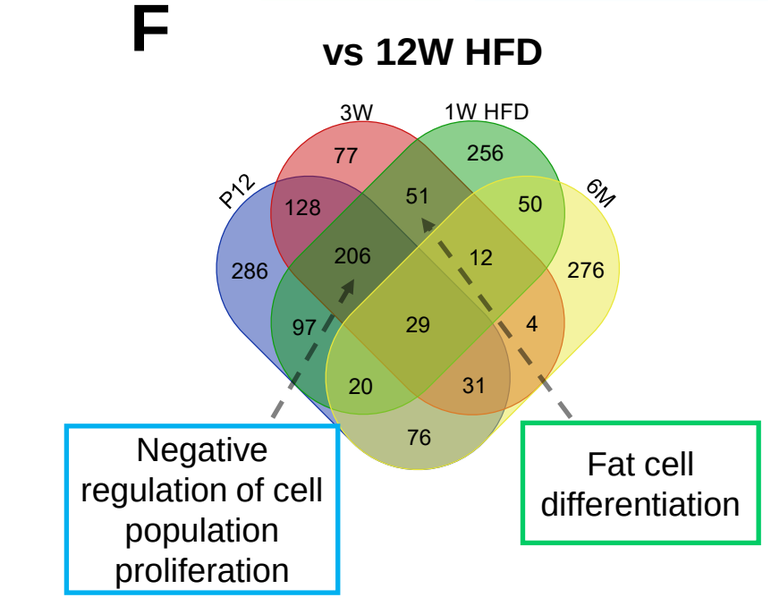
F
vs 12W HFD
3W
1W HFD
P12
6M
77
256
128
51
50
286
206
12
276
97
29
4
20
31
76
Negative regulation of cell population proliferation
Fat cell differentiation

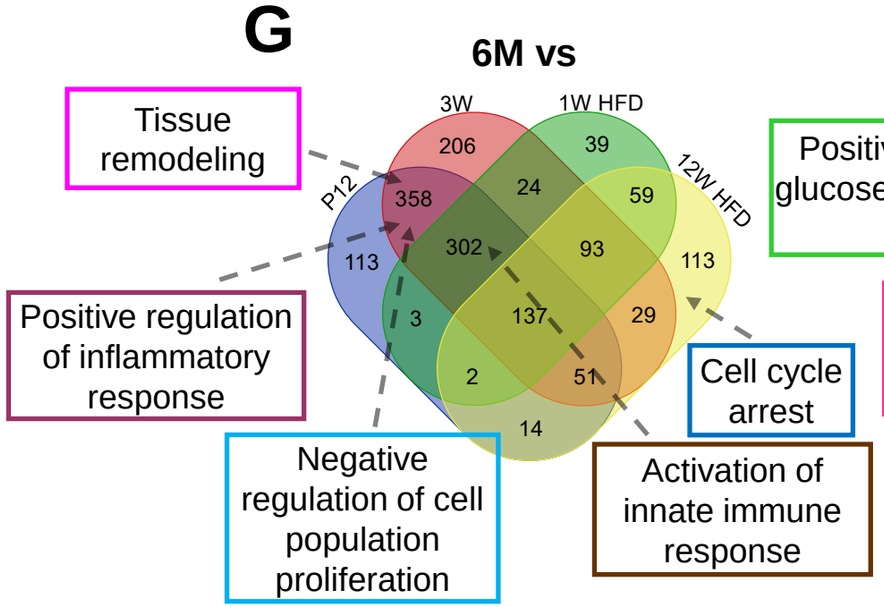
G
6M vs
Tissue remodeling
3W
1W HFD
12W HFD
P12
206
39
358
24
59
302
93
113
113
3
137
29
2
51
14
Positive regulation of inflammatory response
Negative regulation of cell population proliferation
Cell cycle arrest
Activation of innate immune response

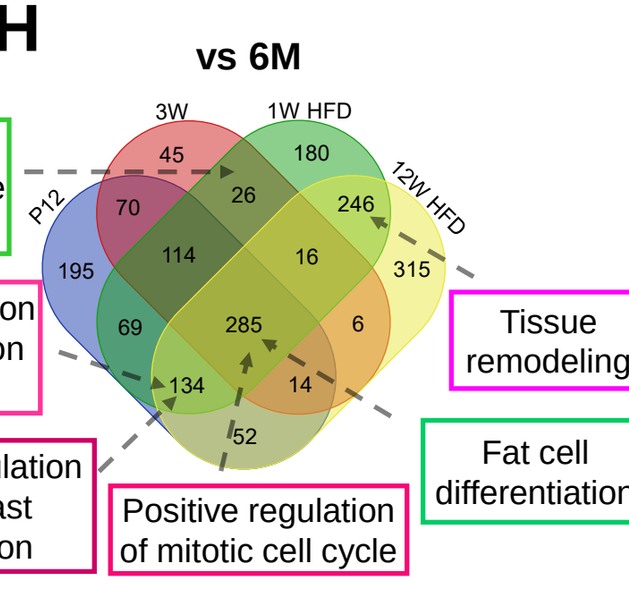
H
vs 6M
Positive regulation of glucose transmembrane transport
3W
1W HFD
12W HFD
P12
45
180
70
26
246
195
114
16
315
69
285
6
134
14
52
Positive regulation of cell population proliferation
Positive regulation of fibroblast proliferation
Positive regulation of mitotic cell cycle
Tissue remodeling
Fat cell differentiation

Figure S2 (Related Figure 2). **Dynamic gene expression profiles of *Tcf21* LCs in mice of different ages and adiposity.** (**A**-**B**) *Tcf21* LCs isolated from WT *Tcf21* LT mice at P12, 3W, 6M, 1W HFD, and 12W HFD were subjected to bulk RNAseq. PCA (**A**) and tSNE (**B**) analyses show the clustering of samples of the same groups. (**C**-**H**) The gene expression profiles of every 2 sample groups were subjected to GSEA to identify biological processes enriched in each sample group compared to every other sample group. Venn diagram shows the overlapping among biological processes enriched in other groups as compared to P12 (**C**), 3W (**D**), 1W HFD (**E**), 12W HFD (**F**), or 6M (**G**), or the overlapping among biological processes enriched in 6M as compared to other groups (**H**). The names of select enriched biological processes are also shown. (**I**) A heatmap shows the expression of select DEGs in *Tcf21* LCs isolated at different time points. Genes were grouped based on their functions and color-coded. Red indicates pro-mitotic genes. Blue indicates anti-mitotic genes. Green indicates pro-adipogenic genes. Orange indicates anti-adipogenic genes. Purple indicates ECM protein and remodeling genes. Yellow indicates inflammatory genes. n=2 for P12 and 6M; n=7 for 3W; n=4 for 1W HFD; n=5 for 12W HFD.

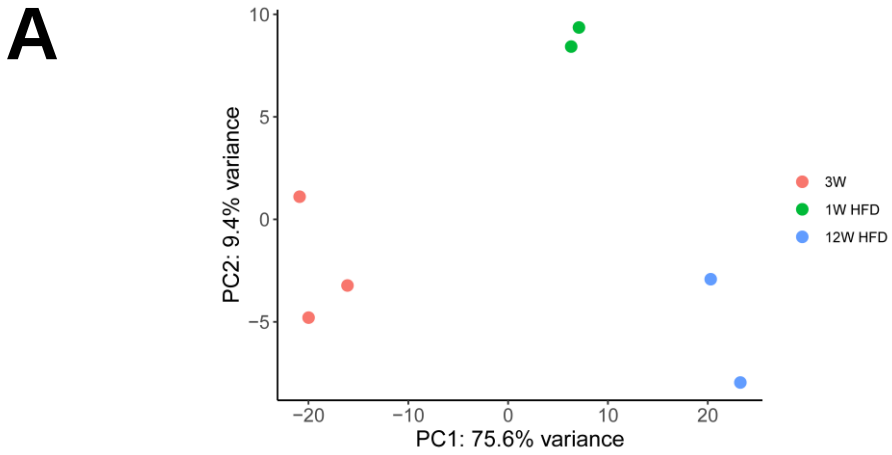
A
PC2: 9.4% variance
PC1: 75.6% variance
3W
1W HFD
12W HFD

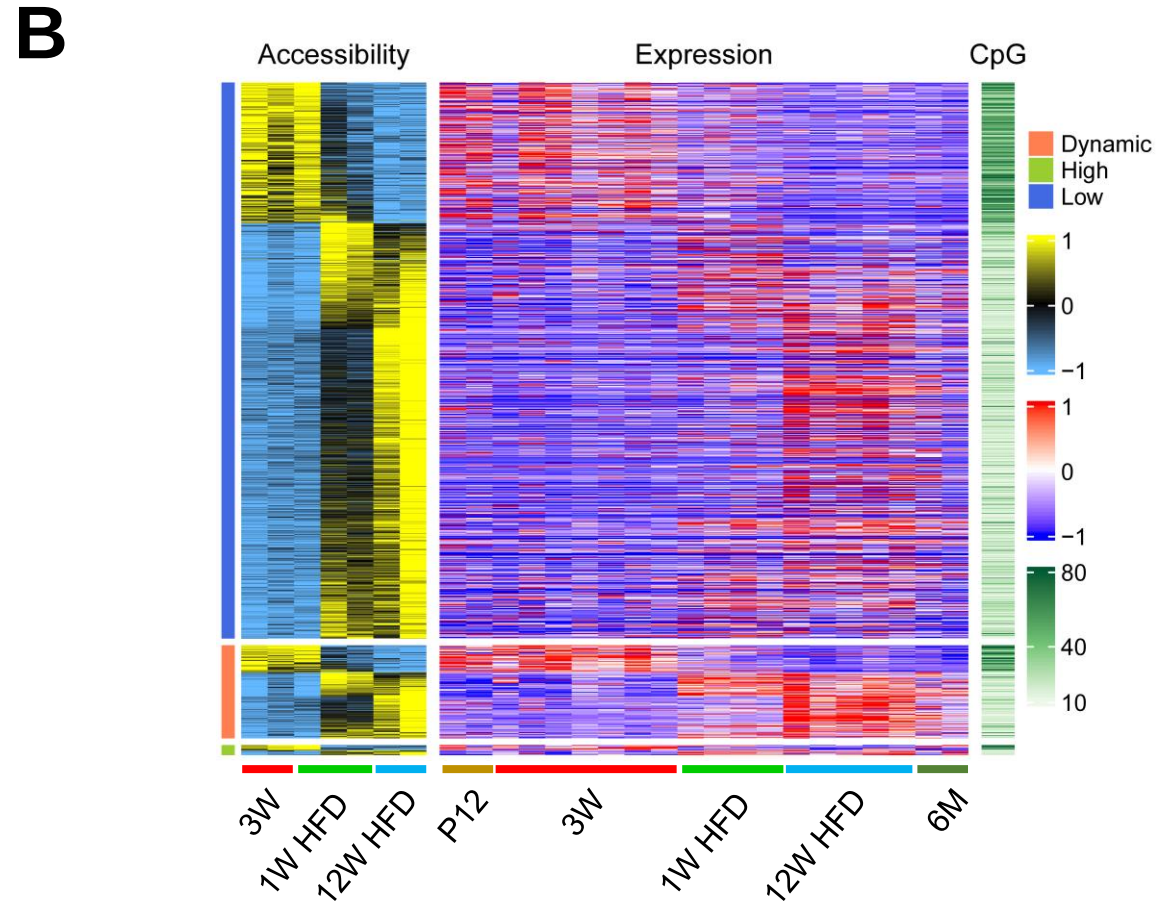
B
Accessibility
Expression
CpG
Dynamic
High
Low
3W
1W HFD
12W HFD
P12
3W
1W HFD
12W HFD
6M

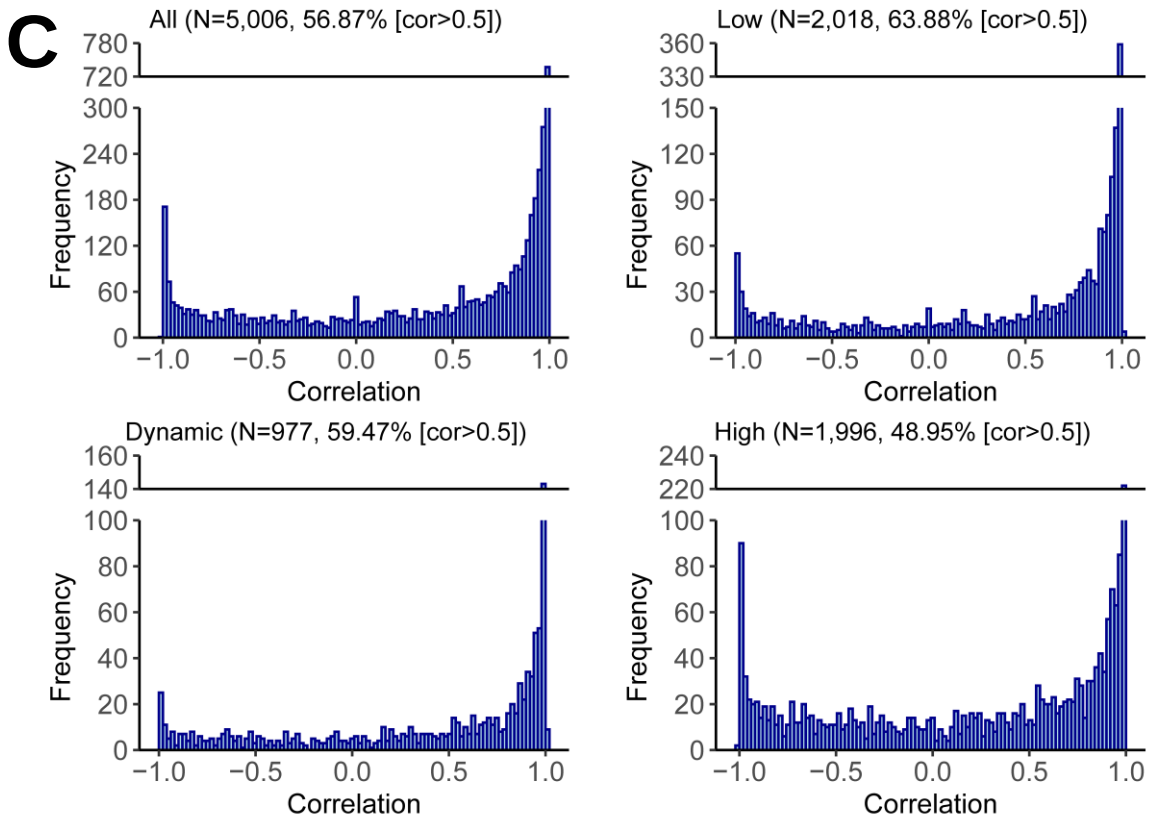
C
All (N=5,006, 56.87% [cor>0.5])
Low (N=2,018, 63.88% [cor>0.5])
Dynamic (N=977, 59.47% [cor>0.5])
High (N=1,996, 48.95% [cor>0.5])
Frequency
Correlation

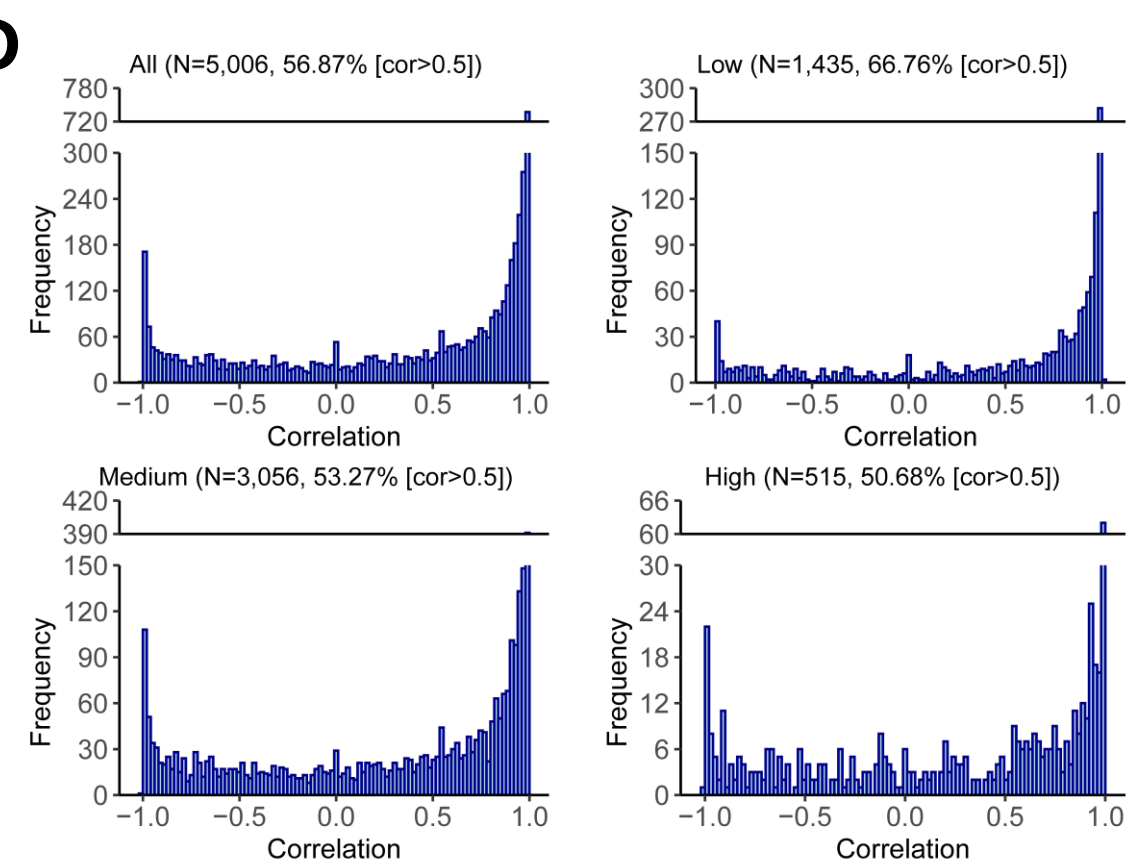
D
All (N=5,006, 56.87% [cor>0.5])
Low (N=1,435, 66.76% [cor>0.5])
Medium (N=3,056, 53.27% [cor>0.5])
High (N=515, 50.68% [cor>0.5])
Frequency
Correlation

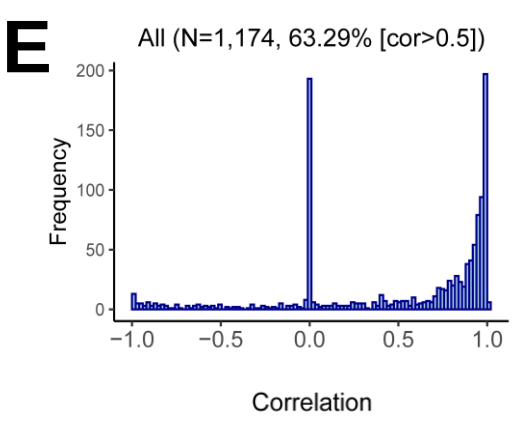
E
All (N=1,174, 63.29% [cor>0.5])
Frequency
Correlation

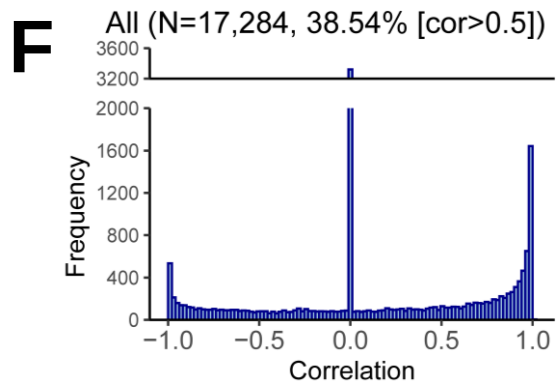
F
All (N=17,284, 38.54% [cor>0.5])
Frequency
Correlation

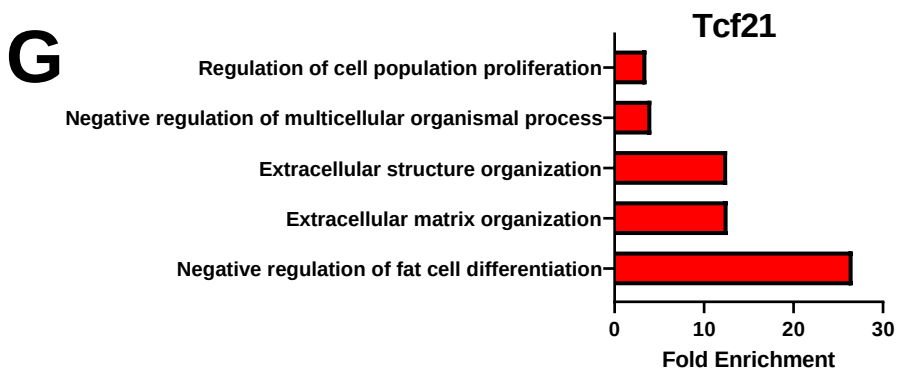
G
Tcf21
Regulation of cell population proliferation
Negative regulation of multicellular organismal process
Extracellular structure organization
Extracellular matrix organization
Negative regulation of fat cell differentiation
Fold Enrichment

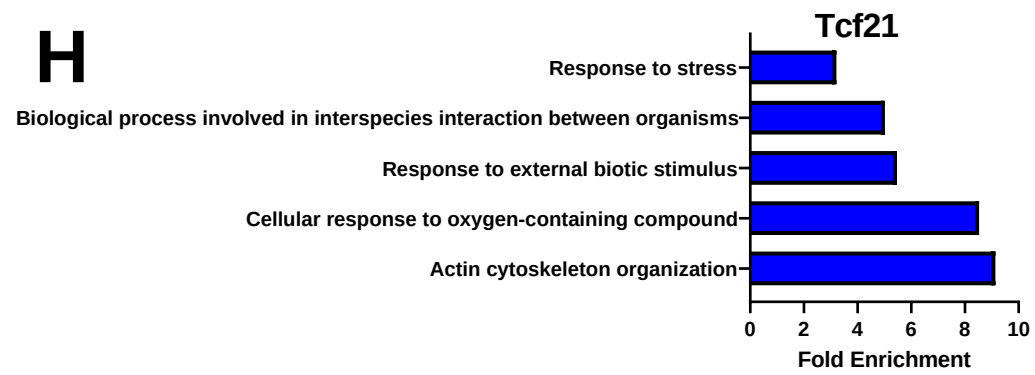
H
Tcf21
Response to stress
Biological process involved in interspecies interaction between organisms
Response to external biotic stimulus
Cellular response to oxygen-containing compound
Actin cytoskeleton organization
Fold Enrichment

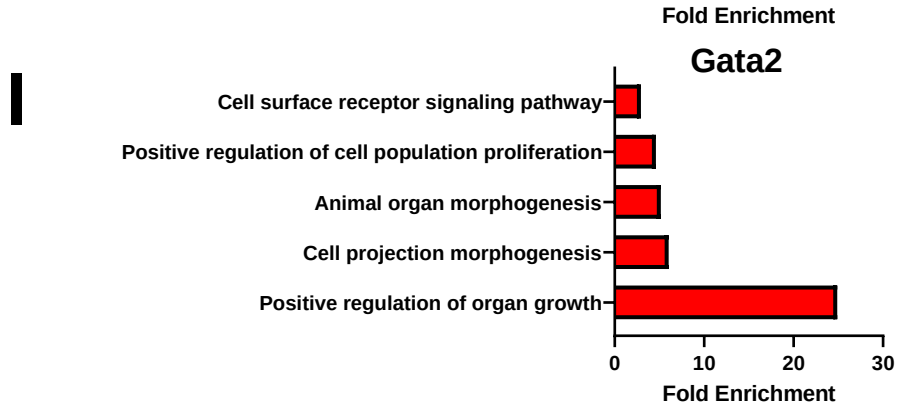
I
Gata2
Cell surface receptor signaling pathway
Positive regulation of cell population proliferation
Animal organ morphogenesis
Cell projection morphogenesis
Positive regulation of organ growth
Fold Enrichment

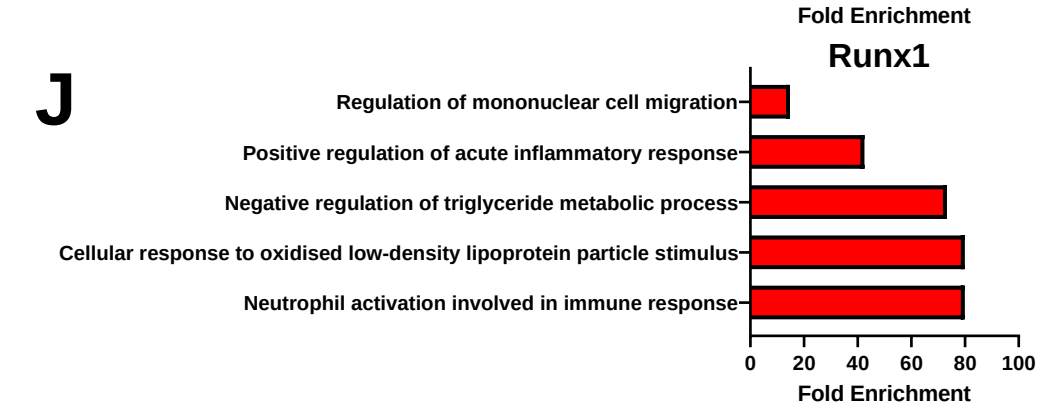
J
Runx1
Regulation of mononuclear cell migration
Positive regulation of acute inflammatory response
Negative regulation of triglyceride metabolic process
Cellular response to oxidised low-density lipoprotein particle stimulus
Neutrophil activation involved in immune response
Fold Enrichment

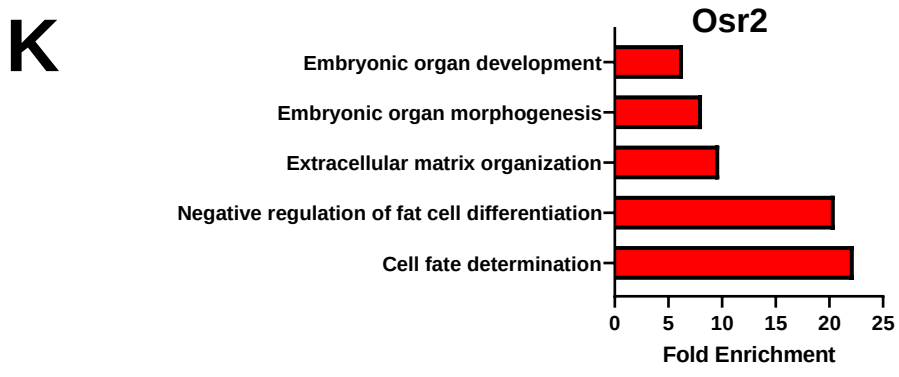
K
Osr2
Embryonic organ development
Embryonic organ morphogenesis
Extracellular matrix organization
Negative regulation of fat cell differentiation
Cell fate determination
Fold Enrichment

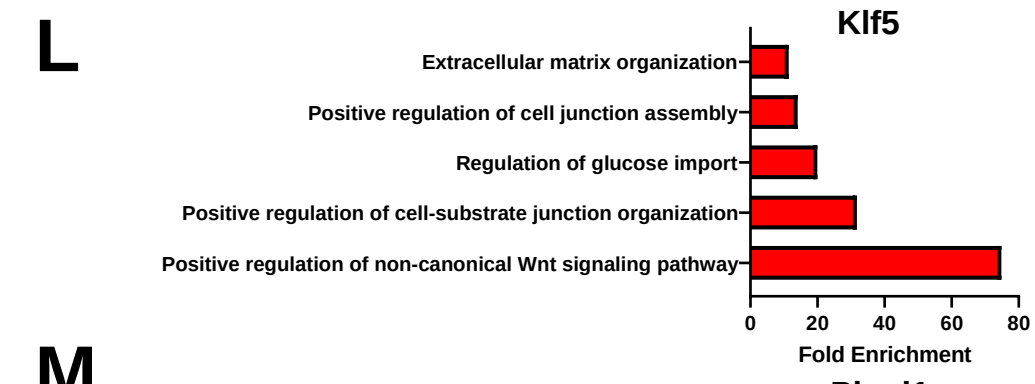
L
Klf5
Extracellular matrix organization
Positive regulation of cell junction assembly
Regulation of glucose import
Positive regulation of cell-substrate junction organization
Positive regulation of non-canonical Wnt signaling pathway
Fold Enrichment

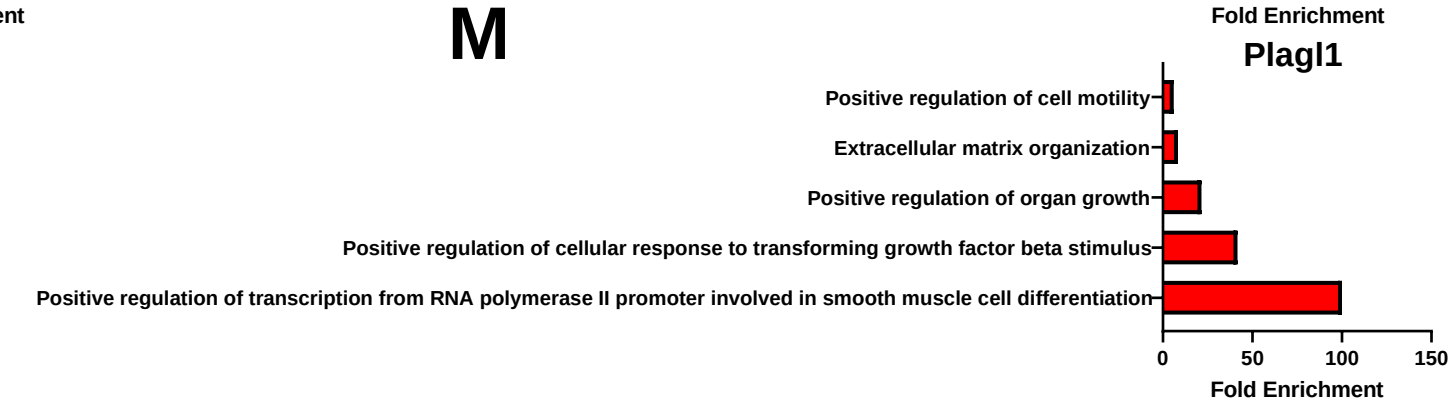
M
Plagl1
Positive regulation of cell motility
Extracellular matrix organization
Positive regulation of organ growth
Positive regulation of cellular response to transforming growth factor beta stimulus
Positive regulation of transcription from RNA polymerase II promoter involved in smooth muscle cell differentiation
Fold Enrichment

Figure S3 (Related Figure 2). **Chromatin remodeling is associated with the dynamic gene expression in *Tcf21* LCs**. (**A**) ATACseq was performed using *Tcf21* LCs isolated at 3W, 1W HFD, and 12W HFD. PCA shows the clustering of samples of the same groups. (**B**) Heatmap shows the promoter accessibility, expression level of corresponding genes, and promoter CpG density of 1,174 DAPs. Genes were divided into three groups based on their promoter accessibility (low, dynamic, and high). The data for accessibility and expression were standardized such that each row (i.e., promoter/gene) has a mean of 0 and a standard deviation of 1 (Z-score). See also Tables S2 and S3. (**C**) 5,006 DEGs were divided into three groups based on their promoter accessibility (low, dynamic, and high). Graphs show the percentages of all DEGs, DEGs with low promoter accessibility, DEGs with dynamic accessibility, and DEGs with high accessibility that have a strong correlation between gene expression and promoter accessibility. (**D**) 5,006 DEGs were divided into three groups based on the CpG density in the promoter (low, medium, and high). Graphs show the percentages of all DEGs, DEGs with low CpG density in the promoter, DEGs with medium CpG density in the promoter, and DEGs with high CpG density in the promoter that have a strong correlation between gene expression and promoter accessibility. (**E**) A graph shows the percentage of 1,174 DAPs that have a high correlation between accessibility and the expression of corresponding genes. (**F**) A graph shows the percentage of 17,284 DADs that have a high correlation between accessibility and the expression of proximal genes. (**G**-**M**) Genes that are up- (**G**) or down- (**H**) regulated by *Tcf21*, or upregulated by *Gata2* (**I**), *Runx1* (**J**), *Osr2* (**K**), *Klf5* (**L**), or *Plagl1* (**M**) were subjected to Gene Ontology analysis to identified enriched biological processes. Select significantly enriched terms are shown in the graphs. n=2, P12 and 6M (RNAseq); n=7, 3W (RNAseq); n=4, 1W HFD (RNAseq); n=5, 12W HFD (RNAseq); n=3, 3W (ATACseq); n=2, 1W and 12W HFD (ATACseq).

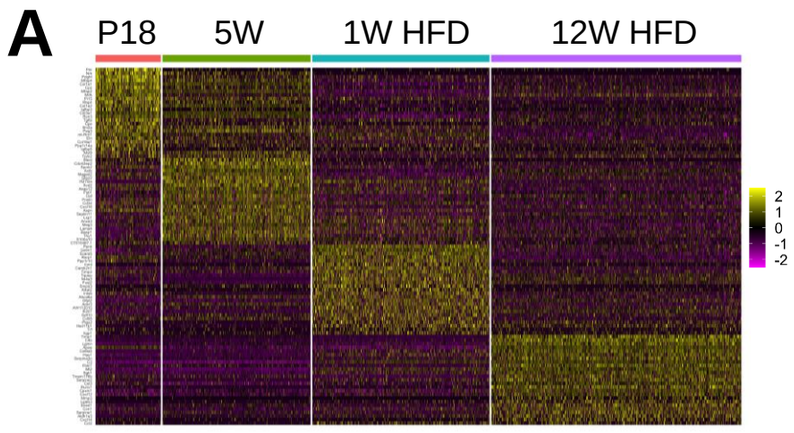
A
P18
5W
1W HFD
12W HFD
2
1
0
-1
-2

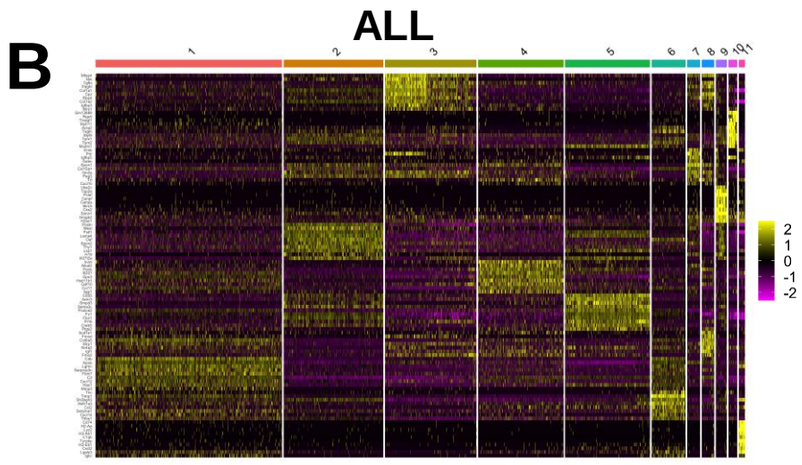
B
ALL
1
2
3
4
5
6
7
8
9
10
11
2
1
0
-1
-2

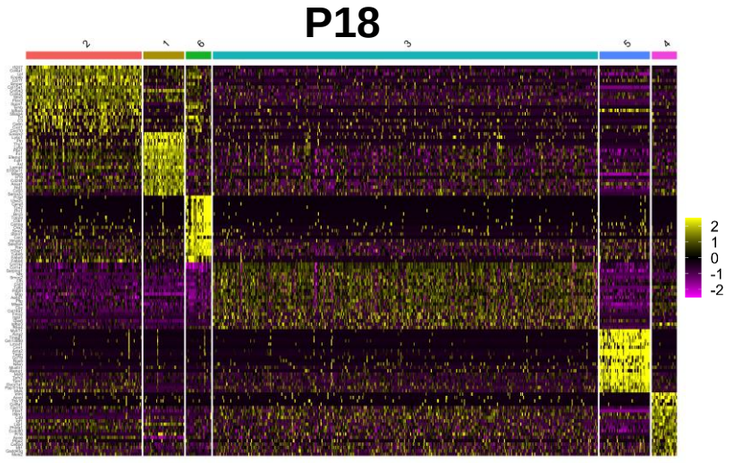
C
P18
2
1
6
3
5
4
2
1
0
-1
-2

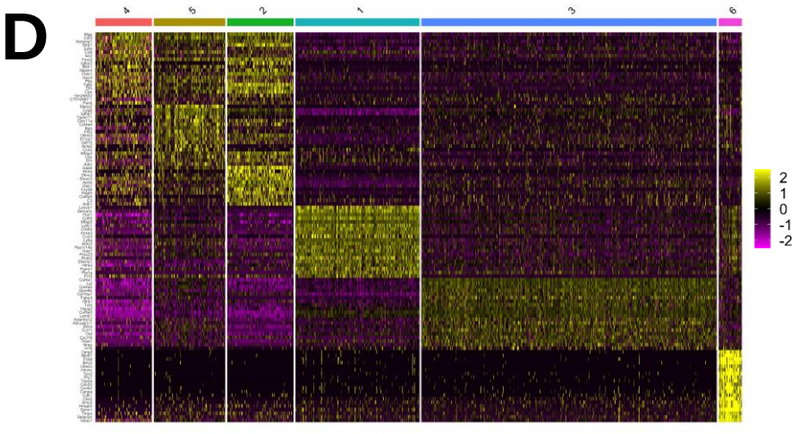
D
5W
4
5
2
1
3
6
2
1
0
-1
-2

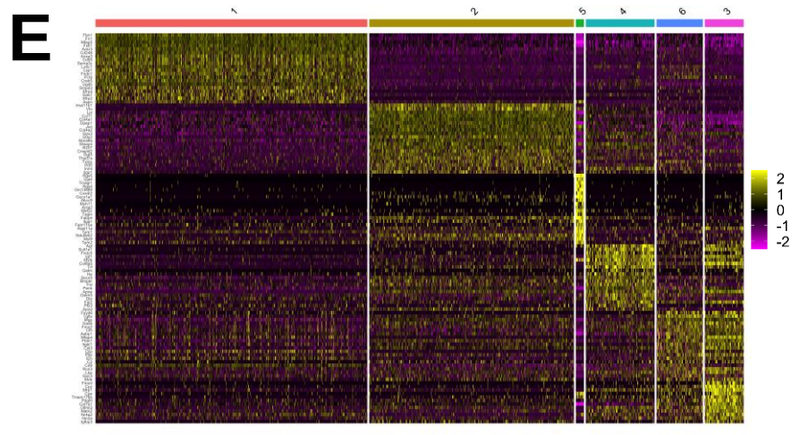
E
1W HFD
1
2
5
4
6
3
2
1
0
-1
-2

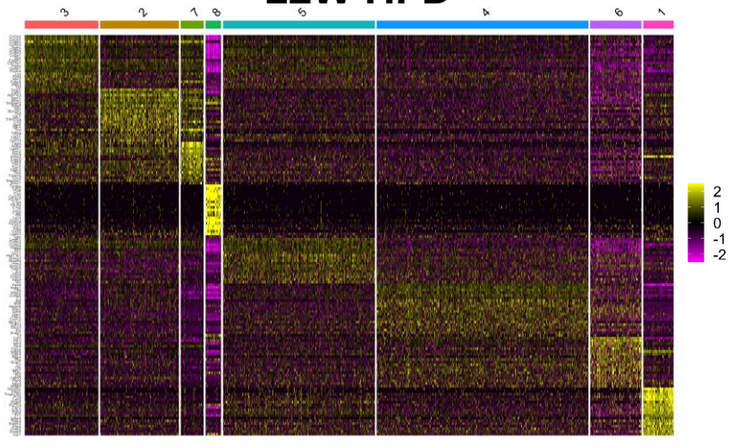
F
12W HFD
3
2
7
8
5
4
6
1
2
1
0
-1
-2

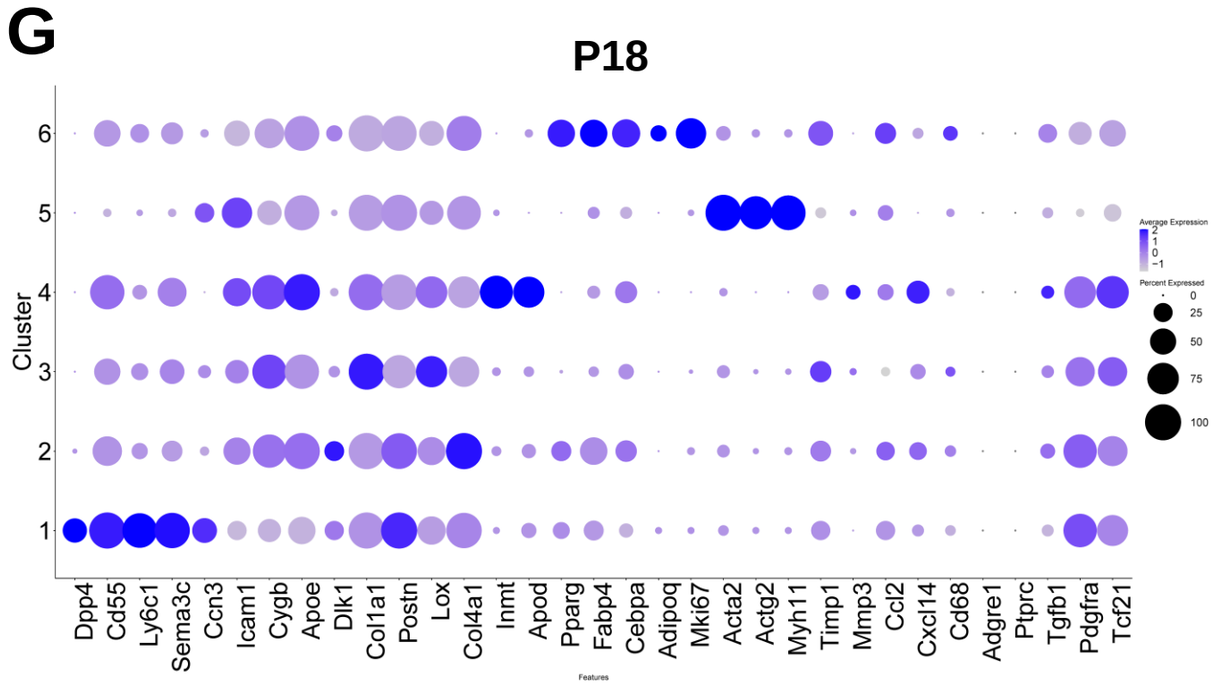
G
P18
Cluster
6
5
4
3
2
1
Dpp4
Cd55
Ly6c1
Sema3c
Ccn3
Icam1
Cygb
Apoe
Dlk1
Col1a1
Postn
Lox
Col4a1
Inmt
Apod
Pparg
Fabp4
Cebpa
Adipoq
Mki67
Acta2
Actg2
Myh11
Timp1
Mmp3
Ccl2
Cxcl14
Cd68
Adgre1
Ptprc
Tgfb1
Pdgfra
Tcf21
Features
Average Expression
2
1
0
−1
Percent Expressed
0
25
50
75
100

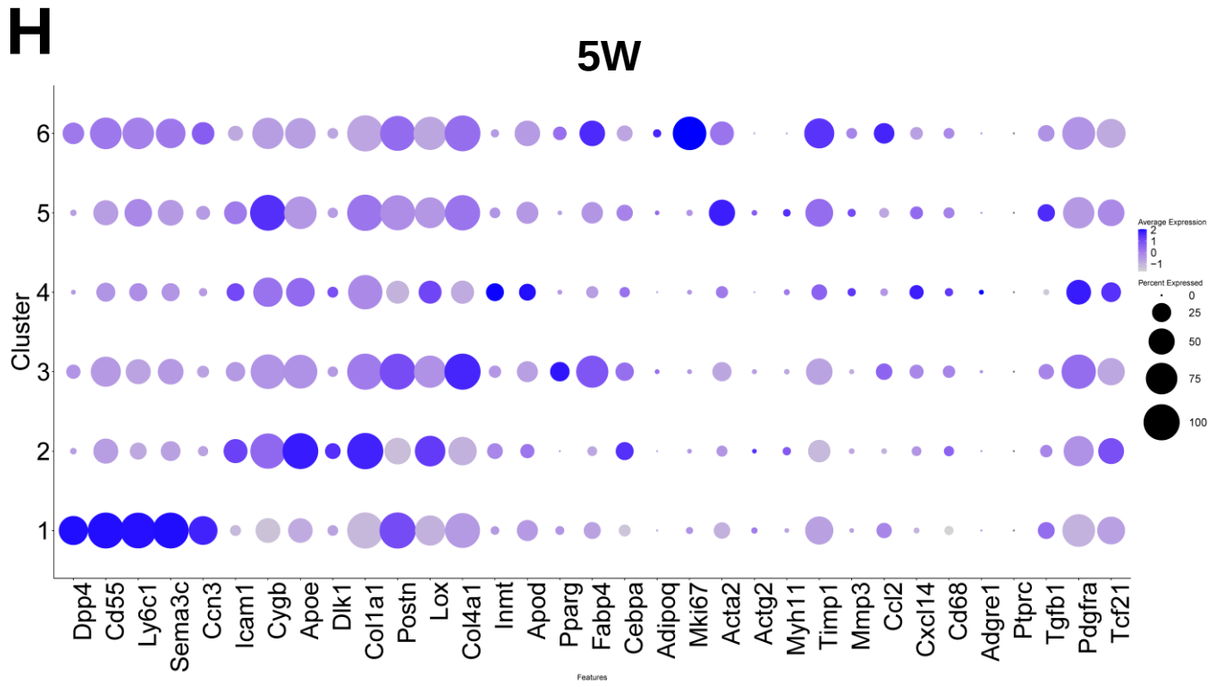
H
5W
Cluster
6
5
4
3
2
1
Dpp4
Cd55
Ly6c1
Sema3c
Ccn3
Icam1
Cygb
Apoe
Dlk1
Col1a1
Postn
Lox
Col4a1
Inmt
Apod
Pparg
Fabp4
Cebpa
Adipoq
Mki67
Acta2
Actg2
Myh11
Timp1
Mmp3
Ccl2
Cxcl14
Cd68
Adgre1
Ptprc
Tgfb1
Pdgfra
Tcf21
Features
Average Expression
2
1
0
−1
Percent Expressed
0
25
50
75
100

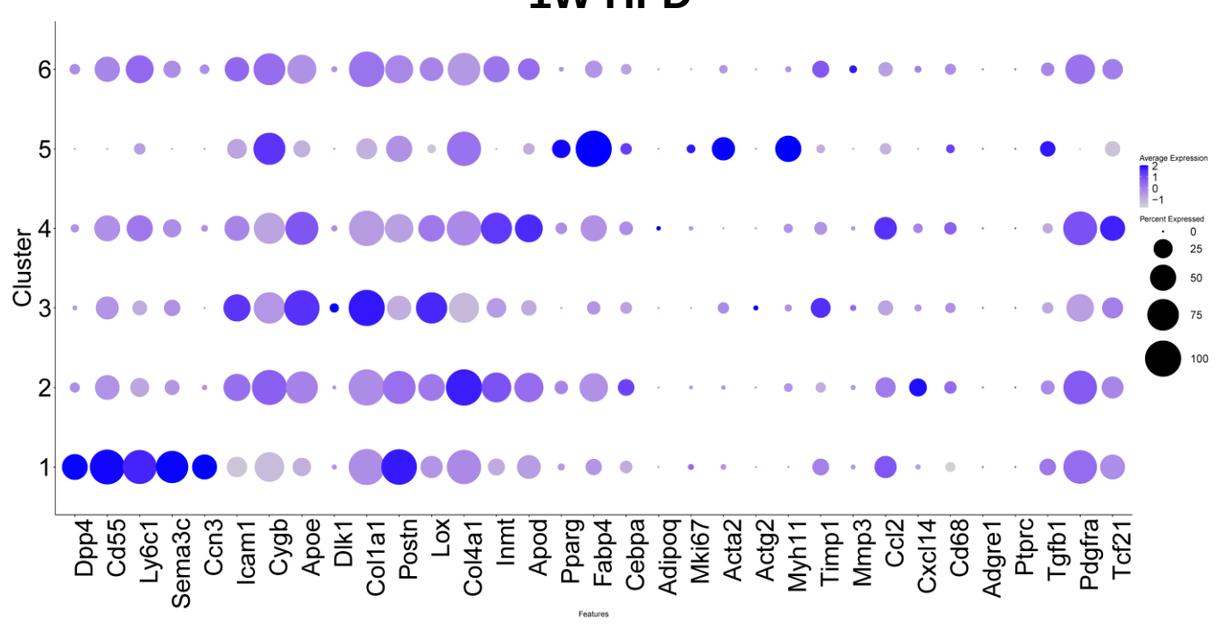
I
1W HFD
Cluster
6
5
4
3
2
1
Dpp4
Cd55
Ly6c1
Sema3c
Ccn3
Icam1
Cygb
Apoe
Dlk1
Col1a1
Postn
Lox
Col4a1
Inmt
Apod
Pparg
Fabp4
Cebpa
Adipoq
Mki67
Acta2
Actg2
Myh11
Timp1
Mmp3
Ccl2
Cxcl14
Cd68
Adgre1
Ptprc
Tgfb1
Pdgfra
Tcf21
Features
Average Expression
2
1
0
−1
Percent Expressed
0
25
50
75
100

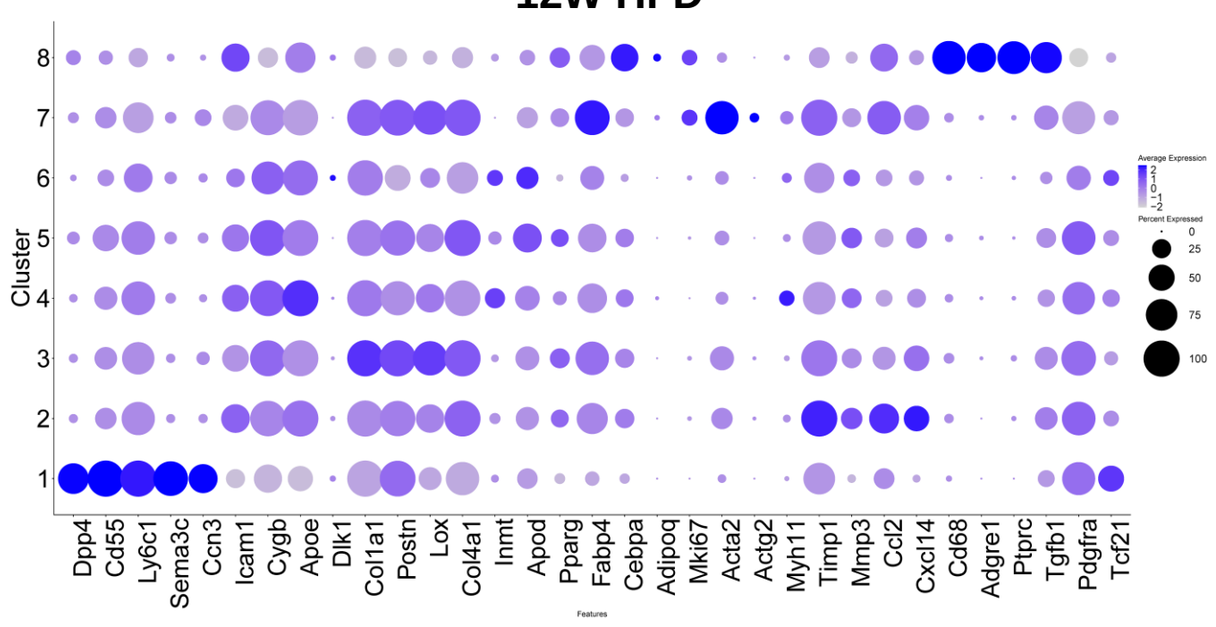
J
12W HFD
Cluster
8
7
6
5
4
3
2
1
Dpp4
Cd55
Ly6c1
Sema3c
Ccn3
Icam1
Cygb
Apoe
Dlk1
Col1a1
Postn
Lox
Col4a1
Inmt
Apod
Pparg
Fabp4
Cebpa
Adipoq
Mki67
Acta2
Actg2
Myh11
Timp1
Mmp3
Ccl2
Cxcl14
Cd68
Adgre1
Ptprc
Tgfb1
Pdgfra
Tcf21
Features
Average Expression
2
1
0
−1
−2
Percent Expressed
0
25
50
75
100

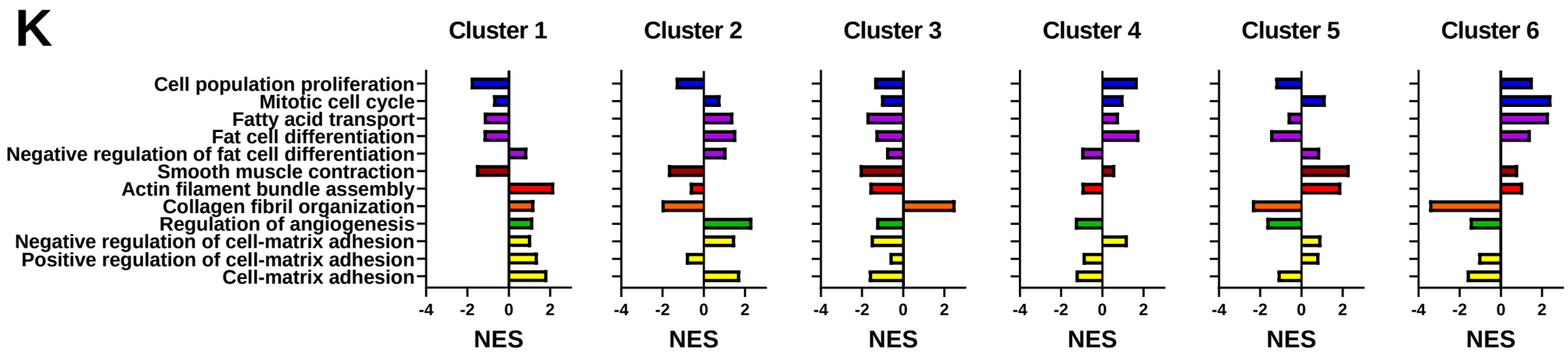
K
Cluster 1
Cluster 2
Cluster 3
Cluster 4
Cluster 5
Cluster 6
Cell population proliferation
Mitotic cell cycle
Fatty acid transport
Fat cell differentiation
Negative regulation of fat cell differentiation
Smooth muscle contraction
Actin filament bundle assembly
Collagen fibril organization
Regulation of angiogenesis
Negative regulation of cell-matrix adhesion
Positive regulation of cell-matrix adhesion
Cell-matrix adhesion
-4
-2
0
2
NES

L
Cluster 1
Cluster 2
Cluster 3
Cluster 4
Cluster 5
Cluster 6
Cluster 7
Cluster 8
Fatty acid transport
Smooth muscle contraction
Mitotic cell cycle
Wound healing
Negative regulation of growth
Collagen fibril organization
Negative regulation of response to stimulus
Inflammatory response
Immune response
Cell-matrix adhesion
Actin filament bundle assembly
Cellular response to decreased oxygen levels
Mesenchymal cell differentiation
-2
0
2
NES

Figure S4 (Related Figure 3). **ScRNAseq analysis identifies the cell type composition of *Tcf21* LCs.** (**A**) ScRNAseq was performed using *Tcf21* LCs isolated at P18, 5W, 1W HFD, and 12W HFD. A heatmap shows the differential gene expression among different sample groups. The expression of top-25 upregulated genes for each sample is included. (**B**) All sample groups were combined and subjected to clustering analysis. A heatmap shows the differential gene expression among different clusters. The expression of top-10 upregulated genes for each cluster is included. (**C**-**F**) Cells in each sample group were subjected to clustering analysis. Heatmaps show the differential gene expression among different clusters at P18 (**C**), 5W (**D**), 1W HFD (**E**), and 12W HFD (**F**). The expression of top-20 upregulated genes for each cluster is included. (**G**-**J**) Dot plots show the expression of select genes in different clusters at P18 (**G**), 5W (**H**), 1W HFD (**I**), and 12W HFD (**J**). (**K**-**L**) The NES of representative biological processes enriched in different clusters identified at P18 (**K**) and 12W HFD (**L**) by GSEA.

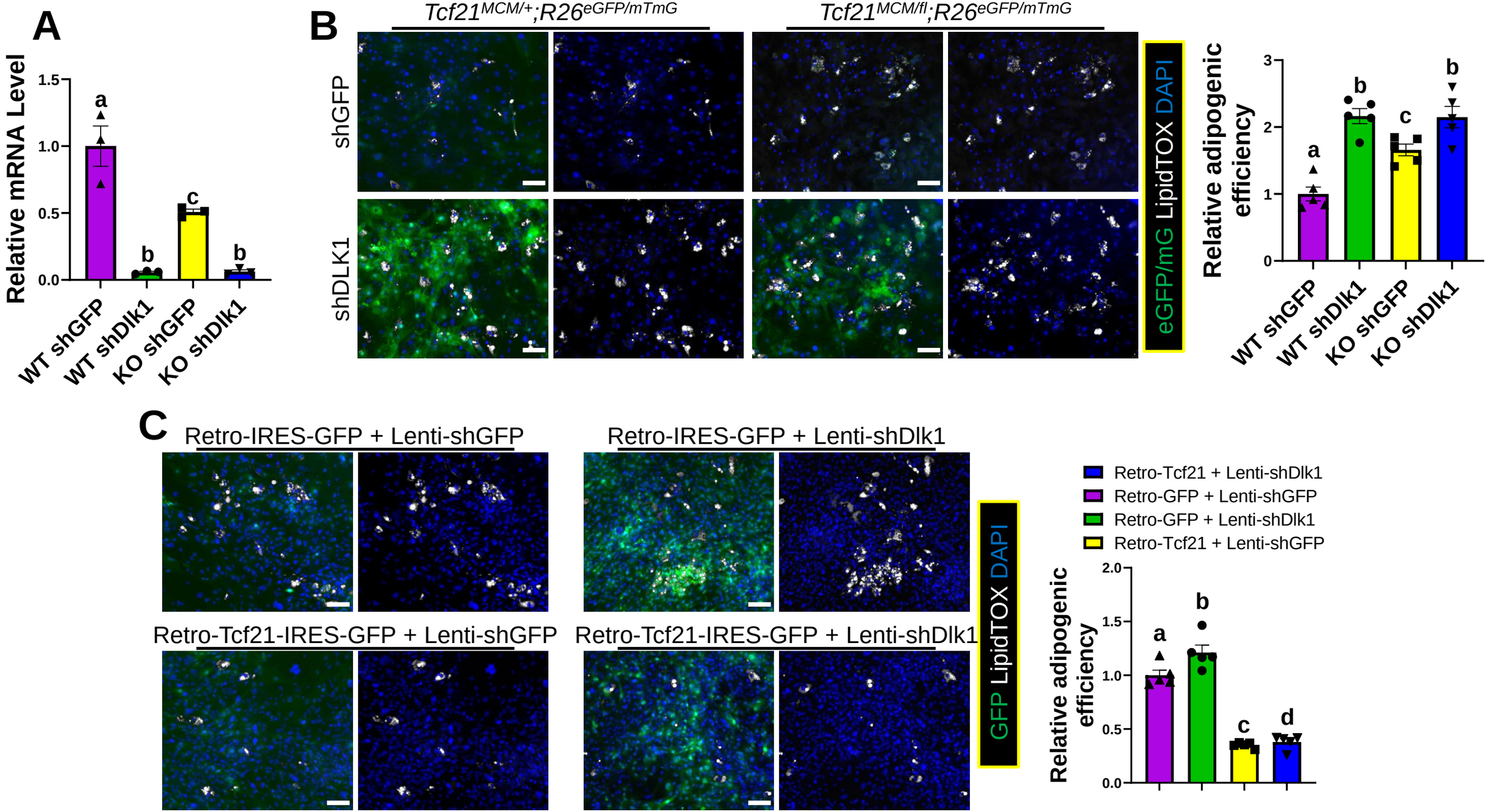
A
Relative mRNA Level
1.5
1.0
0.5
0.0
a
b
c
b
WT shGFP
WT shDlk1
KO shGFP
KO shDlk1
B
Tcf21MCM/+;R26eGFP/mTmG
Tcf21MCM/fl;R26eGFP/mTmG
shGFP
shDLK1
eGFP/mG LipidTOX DAPI
Relative adipogenic efficiency
3
2
1
0
a
b
c
b
WT shGFP
WT shDlk1
KO shGFP
KO shDlk1
C
Retro-IRES-GFP + Lenti-shGFP
Retro-IRES-GFP + Lenti-shDlk1
Retro-Tcf21-IRES-GFP + Lenti-shGFP
Retro-Tcf21-IRES-GFP + Lenti-shDlk1
GFP LipidTOX DAPI
Retro-Tcf21 + Lenti-shDlk1
Retro-GFP + Lenti-shGFP
Retro-GFP + Lenti-shDlk1
Retro-Tcf21 + Lenti-shGFP
Relative adipogenic efficiency
2.0
1.5
1.0
0.5
0.0
a
b
c
d

Figure S5 (Related Figure 6). ***Tcf21*** **inhibits** ***Tcf21*** **LC adipogenic efficiency through promoting** ***Dlk1*** **expression.** (**A**) The expression of *Dlk1* in WT and KO *Tcf21* LCs treated with Lenti-shGFP or Lenti-shDlk1 was measured by realtime PCR. n=3; unpaired *t*-test. (**B**) *Tcf21* LCs isolated from 3W WT and KO mice were treated with Lenti-shGFP or Lenti-shDlk1 and induced for adipogenesis followed by LipidTOX staining to quantify the adipogenic efficiency. Scale bar=50μm. n=5; one-way ANOVA. (**C**) WT *Tcf21* LCs were treated with indicated viruses and induced for adipogenesis followed by LipidTOX staining to quantify the adipogenic efficiency. Scale bar=50μm. n=5; one-way ANOVA. Different letters indicate significant differences ($p<0.05$). Data are represented as mean ± SEM.

A

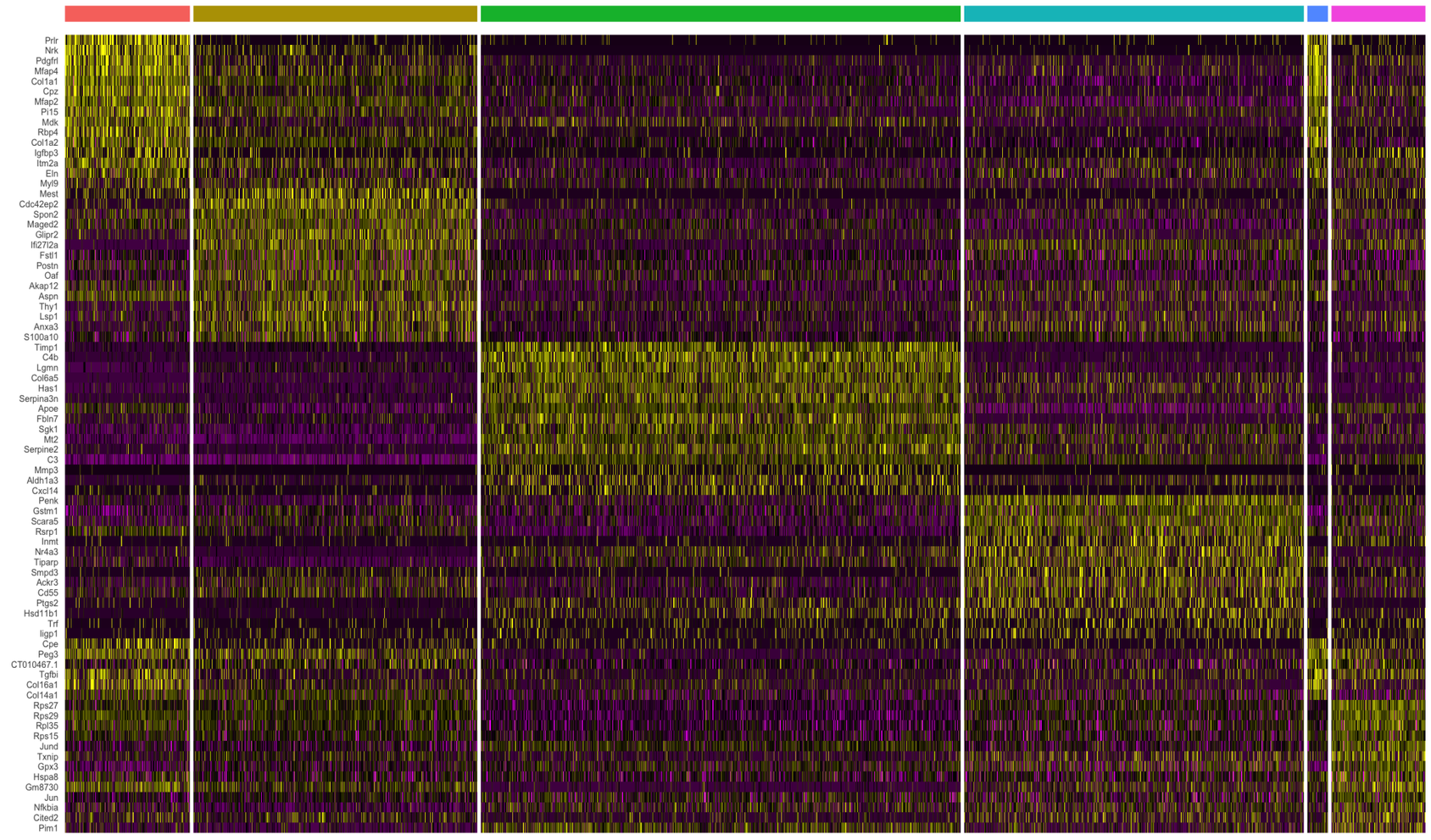
WT P18
WT 5W
WT 12W HFD
WT 1W HFD
KO P18
KO 5W
Prlr
Nrk
Pdgfrl
Mfap4
Col1a1
Cpz
Mfap2
Pi15
Mdk
Rbp4
Col1a2
Igfbp3
Itm2a
Eln
Myl9
Mest
Cdc42ep2
Spon2
Maged2
Glipr2
Ifi27l2a
Fstl1
Postn
Oaf
Akap12
Aspn
Thy1
Lsp1
Anxa3
S100a10
Timp1
C4b
Lgmn
Col6a5
Has1
Serpina3n
Apoe
Fbln7
Sgk1
Mt2
Serpine2
C3
Mmp3
Aldh1a3
Cxcl14
Penk
Gstm1
Scara5
Rsrp1
Inmt
Nr4a3
Tiparp
Smpd3
Ackr3
Cd55
Ptgs2
Hsd11b1
Trf
Iigp1
Cpe
Peg3
CT010467.1
Tgfbi
Col16a1
Col14a1
Rps27
Rps29
Rpl35
Rps15
Jund
Txnip
Gpx3
Hspa8
Gm8730
Jun
Nfkbia
Cited2
Pim1

B

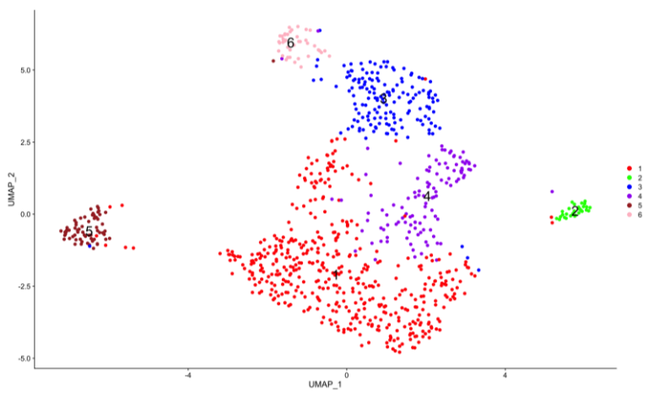
UMAP_1
UMAP_2

C

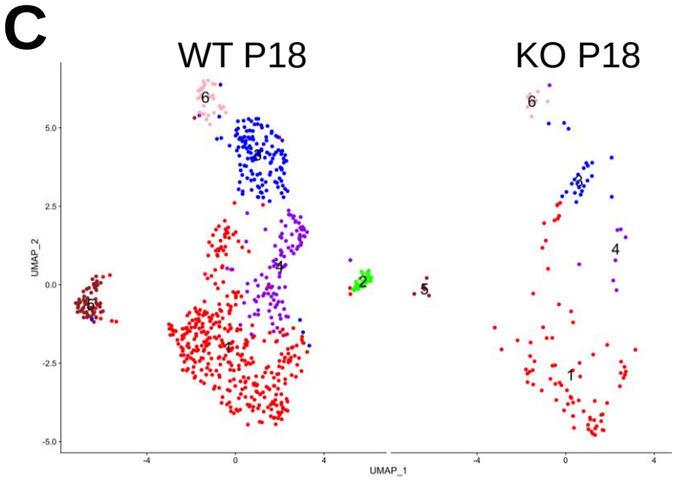
WT P18
KO P18
UMAP_1
UMAP_2

D

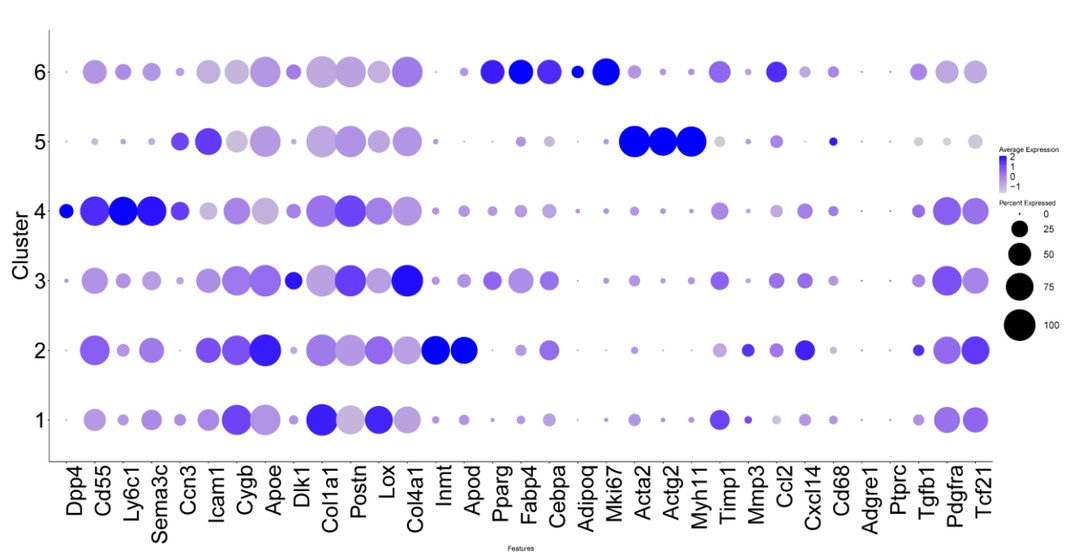
Cluster
Dpp4
Cd55
Ly6c1
Sema3c
Ccn3
Icam1
Cygb
Apoe
Dlk1
Col1a1
Postn
Lox
Col4a1
Inmt
Apod
Pparg
Fabp4
Cebpa
Adipoq
Mki67
Acta2
Actg2
Myh11
Timp1
Mmp3
Ccl2
Cxcl14
Cd68
Adgre1
Ptprc
Tgfb1
Pdgfra
Tcf21
Features
Average Expression
Percent Expressed

E

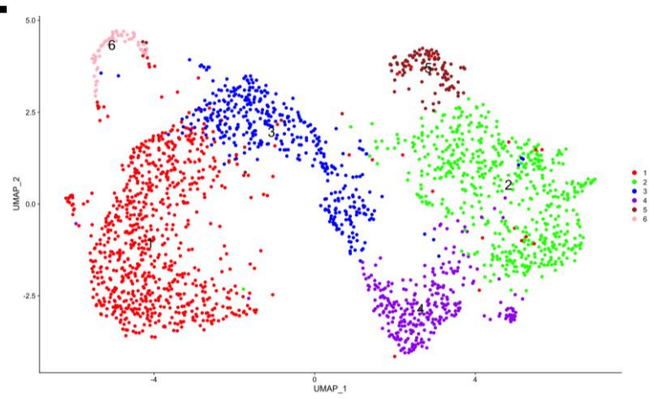
UMAP_1
UMAP_2

F

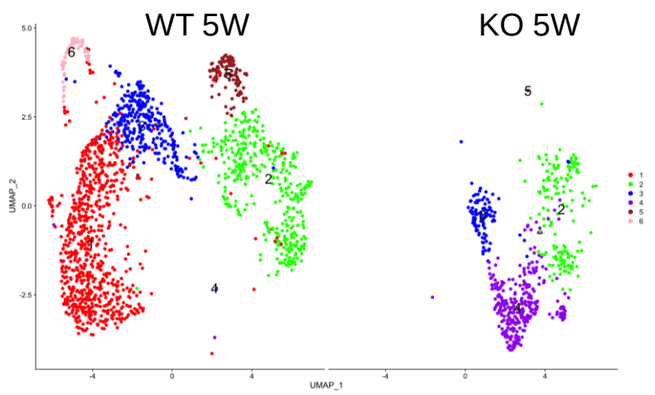
WT 5W
KO 5W
UMAP_1
UMAP_2

G

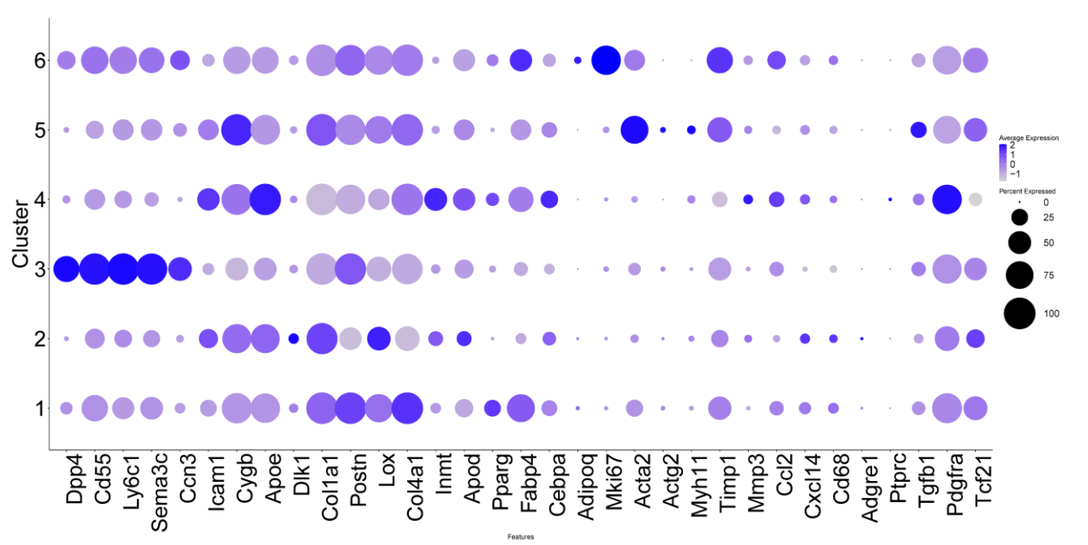
Cluster
Dpp4
Cd55
Ly6c1
Sema3c
Ccn3
Icam1
Cygb
Apoe
Dlk1
Col1a1
Postn
Lox
Col4a1
Inmt
Apod
Pparg
Fabp4
Cebpa
Adipoq
Mki67
Acta2
Actg2
Myh11
Timp1
Mmp3
Ccl2
Cxcl14
Cd68
Adgre1
Ptprc
Tgfb1
Pdgfra
Tcf21
Features
Average Expression
Percent Expressed

Figure S6 (Related Figure 7). **ScRNAseq analysis identifies the cell type composition of *Tcf21* LCs in WT and KO mice.** (**A**) *Tcf21* LCs isolated from WT and KO mice at P18, 5W, 1W HFD (WT only), and 12W (HFD WT only) were subjected to scRNAseq. A heatmap shows the differential gene expression among different samples. The expression of top-15 upregulated genes for each sample is included. (**B**-**D**) Cells from WT and KO P18 mice were combined for clustering analysis (**B-C**). The expression of select genes in different clusters is shown in a dot plot (**D**). (**E**-**G**) Cells from WT and KO 5W mice were combined for clustering analysis (**E-F**). The expression of select genes in different clusters is shown in a dot plot (**G**).

A

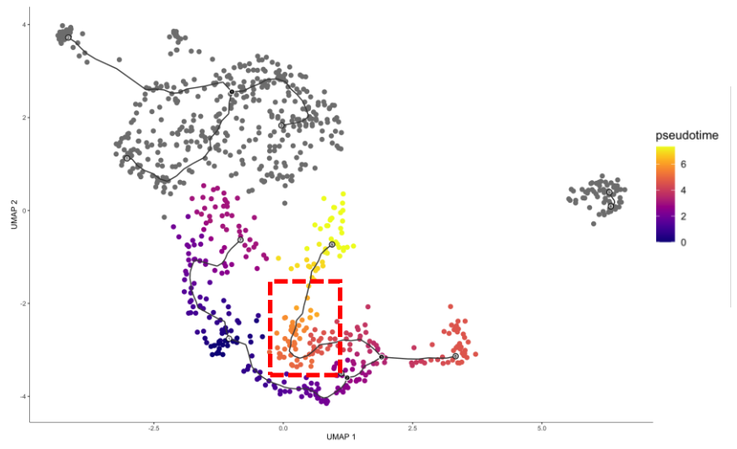

B

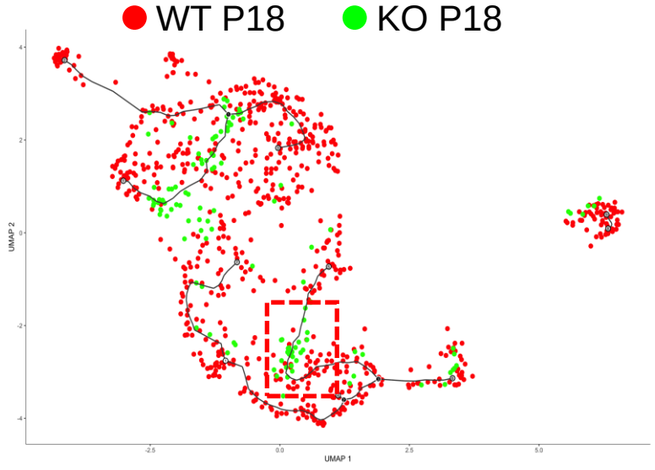

C

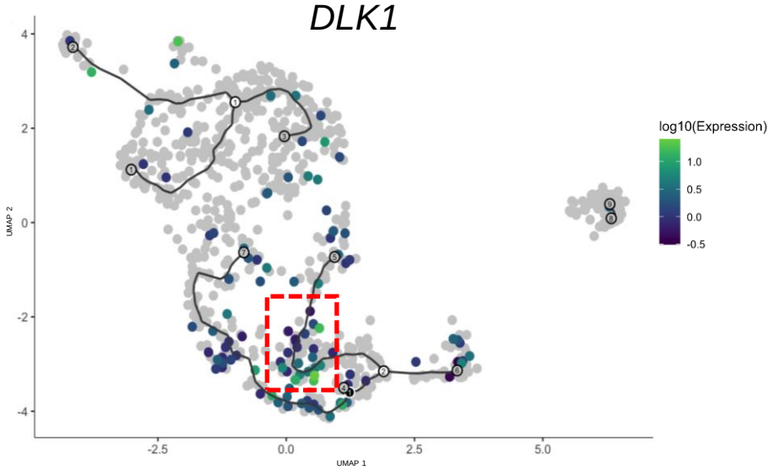

D

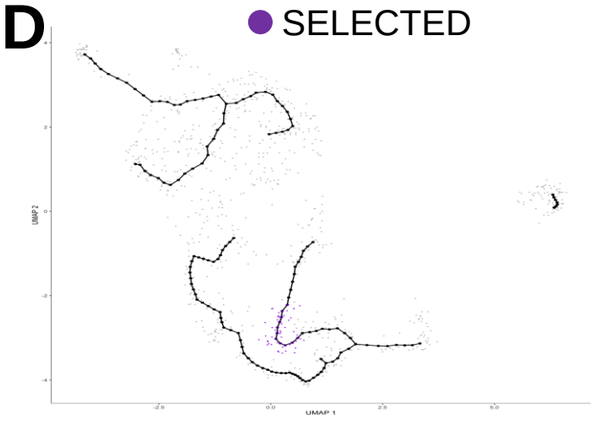

E

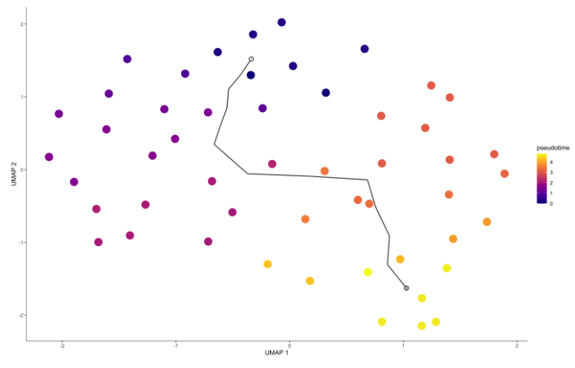

F

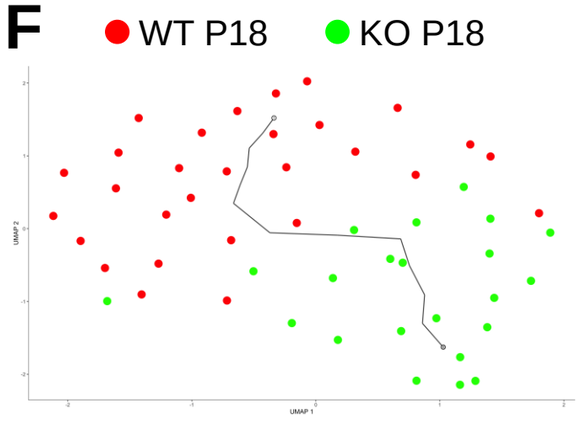

G

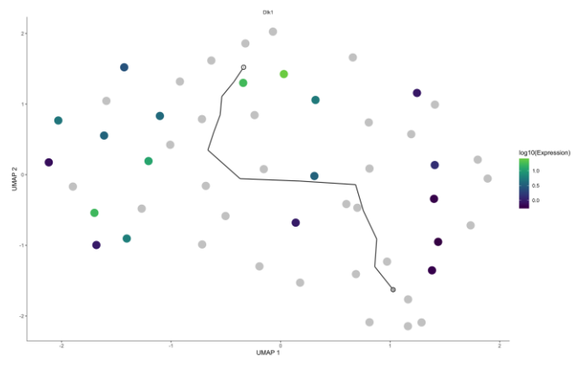

H

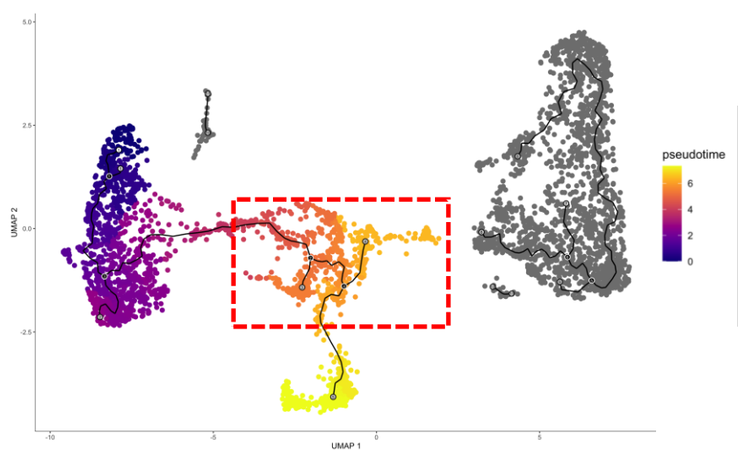

I

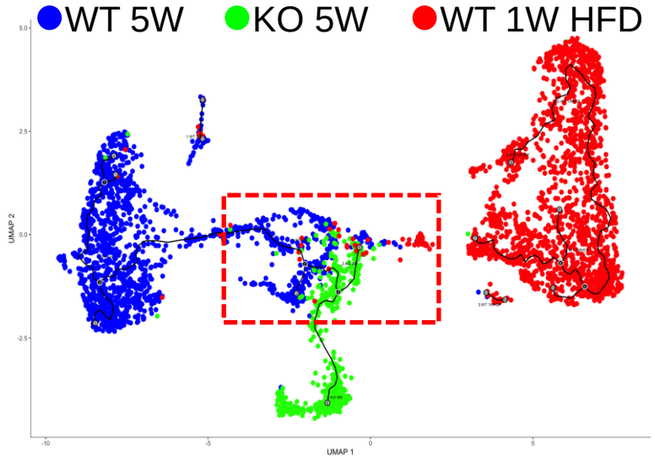

J

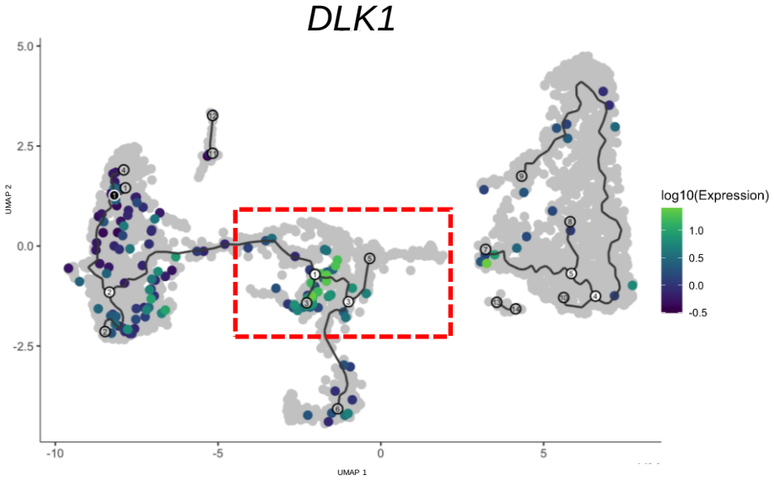

K

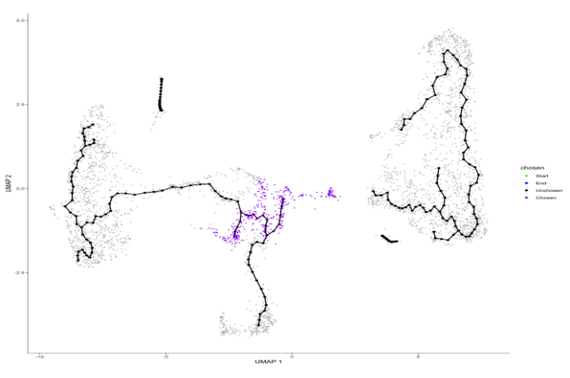

L

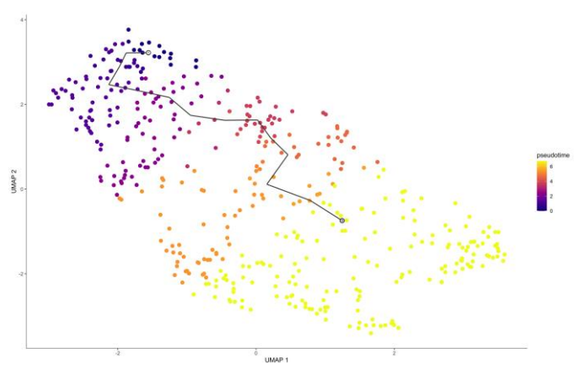

M

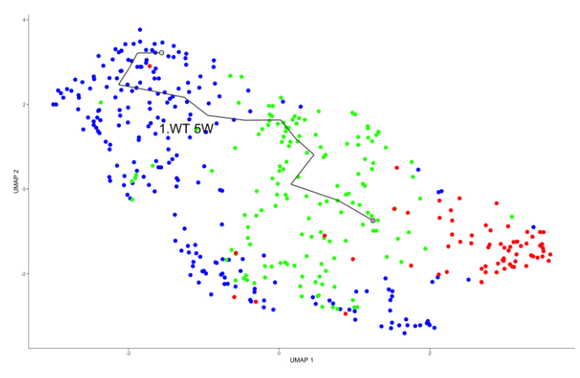

N

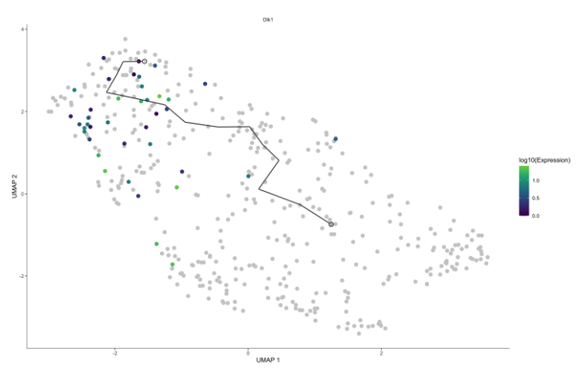

Figure S7 (Related Figure 7)**. Loss of *Tcf21* accelerates the developmental progress of *Tcf21* LCs.** (**A**-**G**) Pseudotime analysis (Monocle 3) of all *Tcf21* LCs isolated from WT and KO P18 mice (**A**) and their distributions on the pseudotime trajectory (**B**). **C** is the UMAP showing the expression of *Dlk1* in individual cells on the pseudotime trajectory. (**D**-**G**) Cells in the red dot-line box in **A**-**C** were selected for further pseudotime analysis. Selected cells are highlighted in purple in **D**. **E** shows the pseudotime trajectory of selected cells. **F** shows the distribution of selected cells from WT and KO P18 mice on the pseudotime trajectory. **G** is the UMAP showing the expression of *Dlk1* in selected cells on the pseudotime trajectory. (**H**-**N**) Pseudotime analysis (Monocle 3) of all *Tcf21* LCs isolated from WT and KO 5W mice and WT 1W HFD mice (**H**) and their distributions on the pseudotime trajectory (**I**). **J** is the UMAP showing the expression of *Dlk1* in individual cells on the pseudotime trajectory. (**K**-**N**) Cells in the red dot-line box in **H**-**J** were selected for further pseudotime analysis. Selected cells are highlighted in purple in **K**. **L** shows the pseudotime trajectory. **M** shows the distribution of selected cells from WT and KO 5W mice and WT 1W HFD mice on the pseudotime trajectory. **N** is the UMAP showing the expression of *Dlk1* in selected cells on the pseudotime trajectory.